

DESIGN RECOMMENDATIONS FOR
STEEL-REINFORCED CONCRETE (SRC)
COUPLING BEAMS

CHRISTOPHER J. MOTTER
JOHN W. WALLACE

UNIVERSITY OF CALIFORNIA, LOS ANGELES
DEPARTMENT OF CIVIL & ENVIRONMENTAL ENGINEERING

DAVID C. FIELDS
JOHN D. HOOPER
RON KLEMENCIC

MAGNUSSON KLEMENCIC ASSOCIATES, INC.

SPONSOR:



CHARLES PANKOW
FOUNDATION

Building Innovation through Research

Design Recommendations for Steel-Reinforced Concrete (SRC) Coupling Beams

Christopher J. Motter

Department of Civil and Environmental Engineering
University of California, Los Angeles

David C. Fields

Magnusson Klemencic Associates, Inc.

John D. Hooper

Magnusson Klemencic Associates, Inc.

Ron Klemencic

Magnusson Klemencic Associates, Inc.

John W. Wallace

Department of Civil and Environmental Engineering
University of California, Los Angeles

Report to Charles Pankow Foundation
School of Engineering and Applied Science
University of California, Los Angeles

December 2013 Final Draft

EXECUTIVE SUMMARY

Design and modeling recommendations for steel reinforced concrete (SRC) coupling beams are provided for both code-based (prescriptive) design and alternative (non-prescriptive) design accomplished using linear response spectrum or nonlinear response history analyses. SRC coupling beams provide an alternative to reinforced concrete coupling beams, diagonally-reinforced for shorter spans and longitudinally-reinforced for longer spans, and offer potential advantages of reduced section depth, reduced congestion at the wall boundary region leading to cost savings, improved degree of coupling for a given beam depth, and improved deformation capacity. The recommendations incorporate information from the 2010 AISC Seismic Provisions, which are primarily based on beam tests of shear-yielding members, as well as new information obtained from four large-scale tests of flexure-yielding SRC coupling beams without face bearing plates and auxiliary transfer bars, which are required by the 2010 AISC Seismic Provisions. For prescriptive design, recommendations are provided to determine the required embedment length of the structural steel member into the reinforced concrete wall, effective coupling beam stiffness, nominal (lower bound) and expected (upper bound) flexure and shear strengths, and beam and wall detailing. For alternative (non-prescriptive) design, additional parameters are provided to define the deformation capacity (to complete the backbone relations) and to address cyclic degradation.

ACKNOWLEDGEMENTS

The Charles Pankow Foundation provided funding for the development of this document (Grant No. 02-08). This support is gratefully acknowledged, with special thanks extended to Dr. Robert Tener, former Executive Director of the Charles Pankow Foundation, Mark Perniconi, the current Executive Director of the Charles Pankow Foundation, and Dean Browning, the Project Director for the Charles Pankow Foundation.

Test results included in this document were obtained from laboratory tests conducted in the Structural/Earthquake Engineering Research Laboratory at UCLA. Thanks are extended to Charles Pankow Builders for construction of the test specimens. Material donations from Herrick Steel are also greatly appreciated. Special thanks are extended to Steve Keowen, Alberto Salamanca, and Harold Kasper for their help with the test set-up and testing. Anne Lemnitzer, Chris Segura, Chris Hilson, Ryon Marapao, Luis Herrera, Ian Wallace, Charys Clay, Kelsey Sakamoto, and Estefan Garcia are thanked for their assistance with construction and/or testing. Testing was performed in a laboratory renovated with funds provided by the National Science Foundation under Grant No. 0963183, which is an award funded under the American Recovery and Reinvestment Act of 2009 (ARRA). Any opinions, findings, and conclusions expressed in this material are those of the authors and do not necessarily reflect those of the National Science Foundation.

TABLE OF CONTENTS

EXECUTIVE SUMMARY	iii
ACKNOWLEDGEMENTS	iv
TABLE OF CONTENTS	v
LIST OF SYMBOLS	vi
1. DESIGN AND MODELING RECOMMENDATIONS	1
1.1 Introduction	1
1.2 Organization and Scope	2
2. CODE-BASED (PRESCRIPTIVE) DESIGN GUIDELINES	3
2.1 Expected Material Properties	4
2.2 Flexural Strength	7
2.3 Shear Strength	11
2.4 Effective Stiffness	15
2.5 Embedment Length	21
2.6 Embedment Detailing	24
2.6.1 Wall Longitudinal Reinforcement	24
2.6.2 Wall Boundary Transverse Reinforcement	29
2.6.3 Auxiliary Transfer Bars and Bearing Plates	34
2.7 Concrete Encasement Detailing	36
3. ALTERNATIVE (NON-PRESCRIPTIVE) DESIGN GUIDELINES	38
3.1 Applicability of Prescriptive Design Guidelines	39
3.2 Modeling and Behavior Categories	44
3.3 Wall Demands	49
APPENDIX A. SAMPLE COMPUTATION FOR FLEXURAL STRENGTH	51
APPENDIX B. TEST RESULTS AND BACKBONE MODELING	54
B.1 Summary of Test Parameters	54
B.2 Modeling	55
REFERENCES	66

LIST OF SYMBOLS

A	cross-sectional area
A_1	effective rotational stiffness term used for backbone modeling, expressed as K / M_{pe}
A_2	effective bending stiffness term used for backbone modeling, expressed as $(EI)_{eff} / E_s I_{trans}$
A_f	flange area of steel section
A_s	total area of longitudinal wall reinforcement crossing the embedment length, L_e , of an SRC coupling beam
A_{st}	area of transverse steel reinforcement, provided at a center-to-center spacing of s
A_w	area of steel section resisting shear, taken as the product of the section depth, d , and web thickness, t_w
a	distance from the point of shear load application to the beam-wall or beam-column interface for a cantilever test beam, i.e., the cantilever length
a_1	depth of uniform magnitude (Whitney) stress block, determined as the product of the neutral axis depth, x , and the ACI stress block factor, β_1
B_1	load at yield plateau used for backbone modeling, expressed as M / M_{pe} or $V / V@M_{pe}$
b	width of an SRC coupling beam, taken as the width of concrete encasement
b_f	flange width of steel section
b_w	width (thickness) of a reinforced concrete wall into which the steel section of an SRC coupling beam is embedded
C	resultant compressive force

C_l	strength drop for backbone modeling, expressed as expressed as M / M_{pe} or $V / V@M_{pe}$
C_b	resultant concrete bearing force developed within the embedment zone of an SRC coupling beam, located near the back of the embedded steel section, and acting normal to the flange of the embedded steel section
C_{c1}	resultant compression force in concrete cover, used when computing M_p or M_{pe} using plastic section analysis for an SRC coupling beam
C_{c2}	resultant compression force in concrete at depth of steel flange, used when computing M_p or M_{pe} using plastic section analysis for an SRC coupling beam
C_{c3}	resultant compression force in concrete at depth of steel web, used when computing M_p or M_{pe} using plastic section analysis for an SRC coupling beam
C_f	resultant concrete bearing force developed within the embedment zone of an SRC coupling beam, located near the front of the embedded steel section, and acting normal to the flange of the embedded steel section
C_{sf}	resultant tension force in web of steel section, used when computing M_p or M_{pe} using plastic section analysis for an SRC coupling beam
C_{sw}	resultant tension force in web of steel section, used when computing M_p or M_{pe} using plastic section analysis for an SRC coupling beam
c	the wall clear cover in the long direction measured from the edge of the wall to the outside of the boundary transverse reinforcement if present or to the outside of the outermost longitudinal reinforcement if boundary transverse reinforcement is not present
D_l	for backbone modeling, the chord rotation (in radians) over which the strength drop, C_l , occurs
d	depth (height) of steel section

d_c	depth of longitudinal tension reinforcement in an SRC coupling beam cross-section, measured from the extreme concrete compression fiber to the center of the longitudinal tension reinforcement
$(EI)_{eff}$	effective elastic bending stiffness of an SRC coupling beam
$(EA)_{eff}$	effective elastic shear stiffness of an SRC coupling beam
E	modulus of elasticity
E_c	modulus of elasticity of concrete
E_s	modulus of elasticity of steel
F_y	specified minimum yield strength of structural steel
F_{ye}	expected yield strength of structural steel
f_c	concrete compressive stress
f'_c	specified compressive strength of concrete
f'_{ce}	expected compressive strength of concrete
f_y	specified yield strength of reinforcement
f_{ye}	expected yield strength of reinforcement
G_s	shear modulus of steel
h	the overall section depth of an SRC coupling beam, taken as the section height of concrete encasement
I	moment of inertia
I_{eff}	effective moment of inertia of an SRC coupling beam, the computation of which includes a modification factor, k , to account for shear deformations when modeling shear stiffness as rigid

$I_{g,c}$	moment of inertia of a gross reinforced concrete section, neglecting the impact of reinforcement (i.e., not considering a transformed section)
$I_{g,s}$	moment of inertia of a steel section, neglecting the impact of reinforced concrete encasement for an SRC coupling beam
I_{trans}	moment of inertia of an SRC coupling beam computed using a transformed section, with concrete in compression transformed into an equivalent area of steel based on the modular ratio of steel to concrete, and neglecting concrete tensile strength, i.e., neglecting cracked concrete
K	stiffness of rotational springs located at the beam-wall interfaces of an SRC coupling beam which are used to model slip/extension, with the stiffness expressed in units of interface moment per radian or per unit chord rotation
k	a modification factor used when computing an effective moment of inertia, I_{eff} , for a steel or SRC coupling beam to account for shear deformations when modeling shear stiffness as rigid
L	coupling beam clear span, measured as the distance between the beam-wall interfaces
L_c	coupling beam effective clear span, computed based on increasing the clear span, L , to account for spalling of wall clear cover, c , at the beam-wall interfaces
L_e	embedment length of the steel section of an SRC coupling beam into the structural wall, measured from the beam-wall interface to the embedded end of the steel section
L_{eff}	coupling beam effective clear span, computed based on taking fixity at $L_e/3$ within the beam-wall interfaces in order to account for gapping between the flange of the steel section and the bearing concrete in the portion of the embedment regions near the beam-wall interfaces and the associated lack of fixity at the beam-wall interfaces
M	moment

M_n	nominal flexural strength of an SRC coupling beam, developed at the beam-wall interfaces and computed based on developing M_p at $L_e/3$ inside of the beam-wall interfaces
M_p	nominal plastic flexural strength of an SRC coupling beam cross-section, computed by taking the specified minimum yield strength of structural steel, F_y , as the plastic stress with a uniform magnitude (Whitney) stress block for concrete in compression; concrete tensile strength is neglected and compressive strength is based on the specified value, f'_c
M_{pe}	expected plastic flexural strength of an SRC coupling beam cross-section, computed in the same manner as M_p except for the use of expected material properties, i.e., F_{ye} for steel and f'_{ce} for concrete
M_u	required flexural strength (factored moment)
$M@V_{ne,limit}$	moment developed in an SRC coupling beam at the beam-wall interfaces when the limiting shear strength, $V_{ne,limit}$, of the coupling beam is reached
P_u	required axial strength (factored axial force)
R_y	ratio of the expected yield strength of structural steel, F_{ye} , to the specified minimum yield strength of structural steel, F_y
s	center-to-center spacing of transverse reinforcement
T	resultant tensile force
T_f	resultant tension force in flange of steel section, used when computing M_p or M_{pe} using plastic section analysis for an SRC coupling beam
t_f	flange thickness of steel section
t_w	web thickness of steel section
V	shear force

V_n	nominal shear strength of an SRC coupling beam cross-section, including the contribution of structural steel, concrete, and transverse reinforcement to shear strength
V_{ne}	expected shear strength of an SRC coupling beam cross-section, including the contribution of structural steel, concrete, and transverse reinforcement
$V_{n,limit}$	limiting shear strength of an SRC coupling beam, taken as the smaller of V_{ne} (the expected shear strength) and $V@M_{pe}$ (the coupling beam shear force developed when the expected flexural strength, M_{pe} , is developed at the beam-wall interfaces)
$V_{n,embed}$	the embedment strength of a SRC coupling beam, which is the peak beam shear load that the embedment can resist
V_p	nominal shear strength of a steel section, used to determine the shear strength of an SRC coupling beam
$V@M_n$	SRC coupling beam shear force developed when the nominal flexural strength, M_n , is developed at the beam-wall interfaces and the nominal plastic flexural strength, M_p , is developed at $L_e/3$ inside of the beam-wall interfaces
$V@M_p$	SRC coupling beam shear force developed when the nominal plastic flexural strength, M_p , is developed at the beam-wall interfaces
$V@M_{pe}$	SRC coupling beam shear force developed when the expected flexural strength, M_{pe} , is developed at the beam-wall interfaces
x	neutral axis depth, which is the distance from the extreme compression fiber to the neutral axis
α	the span-to-depth (aspect) ratio of an SRC coupling beam, i.e., the ratio of the clear span, L , to the overall beam height including concrete encasement, h
β_1	ACI stress block factor, taken as the ratio of the uniform magnitude (Whitney) stress block depth, a_1 , to the neutral axis depth, x

ε_c	concrete compressive strain
ε_0	concrete compressive strain corresponding to the specified compressive strength of concrete, f'_c
$\varepsilon_{s,bl}$	maximum tensile strain on wall longitudinal reinforcement at the location of the embedded SRC coupling beam, computed as the mean of the maximum for the building model subjected to the requisite number of base acceleration histories
$\varepsilon_{s,max}$	maximum tensile strain on wall longitudinal reinforcement at the location of the embedded SRC coupling beam, determined analytically based on plane-strain moment-curvature analysis of the structural wall for the observed maximum structural wall loading demands
ε_y	yield strain of wall boundary longitudinal reinforcement
λ	the cross-section shape factor for shear, taken as 1.5 for W-shapes
ρ	the wall boundary longitudinal reinforcement ratio, taken as the total area of wall boundary longitudinal reinforcement divided by the gross concrete area of the wall boundary
θ	coupling beam chord rotation
$\theta_{p,bl}$	maximum plastic rotation of wall at the location of the embedded SRC coupling beam, computed as the mean of the maximum for the building model subjected to the requisite number of base acceleration histories
θ_y	coupling beam chord rotation at yield
$\theta_{y,w}$	wall yield rotation

1. DESIGN AND MODELING RECOMMENDATIONS

1.1 Introduction

Design and modeling recommendations for steel reinforced concrete (SRC) coupling beams are provided for both code-based (prescriptive) design and alternative (non-prescriptive) design accomplished using linear response spectrum or nonlinear response history analyses. SRC coupling beams provide an alternative to reinforced concrete coupling beams, diagonally-reinforced for shorter spans and longitudinally-reinforced for longer spans, and offer potential advantages of reduced section depth, reduced congestion at the wall boundary region leading to cost savings, improved degree of coupling for a given beam depth, and improved deformation capacity. The recommendations incorporate information from the 2010 AISC Seismic Provisions, which are primarily based on beam tests of shear-yielding members, as well as new information obtained from four large-scale tests of flexure-yielding SRC coupling beams without face bearing plates and auxiliary transfer bars, which are required by the 2010 AISC Seismic Provisions. For prescriptive design, recommendations are provided to determine the required embedment length of the structural steel member into the reinforced concrete wall, effective coupling beam stiffness, nominal (lower bound) and expected (upper bound) flexure and shear strengths, and beam and wall detailing. For alternative (non-prescriptive) design, additional parameters are provided to define the deformation capacity (to complete the backbone relations) and to address cyclic degradation.

1.2 Organization and Scope

The design recommendations that follow are organized into two parts, first recommendations for code-based (or prescriptive) design, followed by recommendations for alternative (non-prescriptive) design. For code-based design, recommendations for use with either linear equivalent static or linear response spectrum analysis approaches are provided, whereas for alternative design, recommendations for use with linear response spectrum analysis (for either service-level or code-level design) and nonlinear response history analyses (for service-level or MCE-level design) are provided. Subsections within both the code-based design section and the alternative design section are further divided into recommendations and commentary.

In the 2010 AISC Seismic Provisions, recommendations for steel and SRC coupling beams differ depending on whether the coupling beams are used with ordinary shear walls (satisfying ACI 318-11, excluding Chapter 21) or special shear walls (satisfying ACI 318-11, including Chapter 21). The recommendations in this document were developed specifically for special shear wall systems and specifically for steel reinforced concrete (SRC) coupling beams, although many of the recommendations may also apply to the design of steel coupling beams without concrete encasement.

2. CODE-BASED (PRESCRIPTIVE) DESIGN GUIDELINES

Design recommendations are provided for use with prescriptive design approaches, i.e. use of ASCE 7-10, ACI 318-11, and the 2010 AISC Seismic Provisions. The objective is to provide relatively simple recommendations appropriate for code-prescriptive design approaches to address a range of design issues for reinforced concrete coupling beams with embedded structural steel W-sections, commonly referred to as SRC coupling beams. Guidance and recommendations are provided in the following subsections: (2.1) material properties, (2.2) flexural strength, (2.3) shear strength, (2.4) effective stiffness, (2.5) embedment length, (2.6) embedment detailing, including (2.6.1) wall boundary longitudinal reinforcement, (2.6.2) wall boundary transverse reinforcement, and (2.6.3) auxiliary transfer bars and bearing plates, and (2.7) concrete encasement detailing.

2.1 Expected Material Properties

2.1.1

The expected yield strength of structural steel, F_{ye} , shall be computed as $R_y * F_y$, where F_y is the specified minimum yield strength of structural steel, and R_y is the ratio of the expected yield strength to specified minimum yield strength, determined based on Table A3.1 in Section A3.2 of the 2010 AISC Seismic Provisions (with R_y for hot-rolled structural shapes taken as 1.1 for A992 and A572 and 1.5 for A36). Alternatively, the use of project-specific F_{ye} values is permitted if material test results are available to justify the values used. Values for F_{ye} may differ for the web and the flanges of the steel section (for built-up sections).

C2.1.1

The R_y values for A992, A572, and A36 hot-rolled structural steel shapes recommended by the 2010 AISC Seismic Provisions are consistent with Table 2 of the LATBSDC (2014) document and Table 7.1 of the PEER TBI (2010).

2.1.2

If the expected yield strength of steel reinforcement, f_{ye} , is not known, the use of $f_{ye} = 1.17f_y$ is permitted, where f_y is the specified yield strength of steel reinforcement.

C2.1.2

The use of $f_{ye} = 1.17f_y$ is permitted based on Table 2 of the LATBSDC (2014) document and Table 7.1 of the PEER TBI (2010).

2.1.3

The expected compressive strength of concrete, f'_{ce} , shall be determined based on the specified compressive strength of concrete, f'_c , by using the relationships provided in Table 2.1 and Figure 2.1 (which correspond to Table 5-6 and Figure 5-7, respectively, in Nowak et al, 2008). Alternatively, the use of project-specific f'_{ce} values is permitted, provided a detailed analysis based on material testing sufficiently demonstrates that a project-specific value is reliable.

Table 2.1: Recommended Values for Expected Compressive Strength of Concrete
(Nowak et al, 2008)

f'_c (ksi)	3.0	3.5	4.0	4.5	5.0	5.5	6.0	6.5	7.0	8.0	9.0	10.0	12.0
f'_{ce} / f'_c	1.31	1.27	1.24	1.21	1.19	1.17	1.15	1.14	1.13	1.11	1.1	1.09	1.08

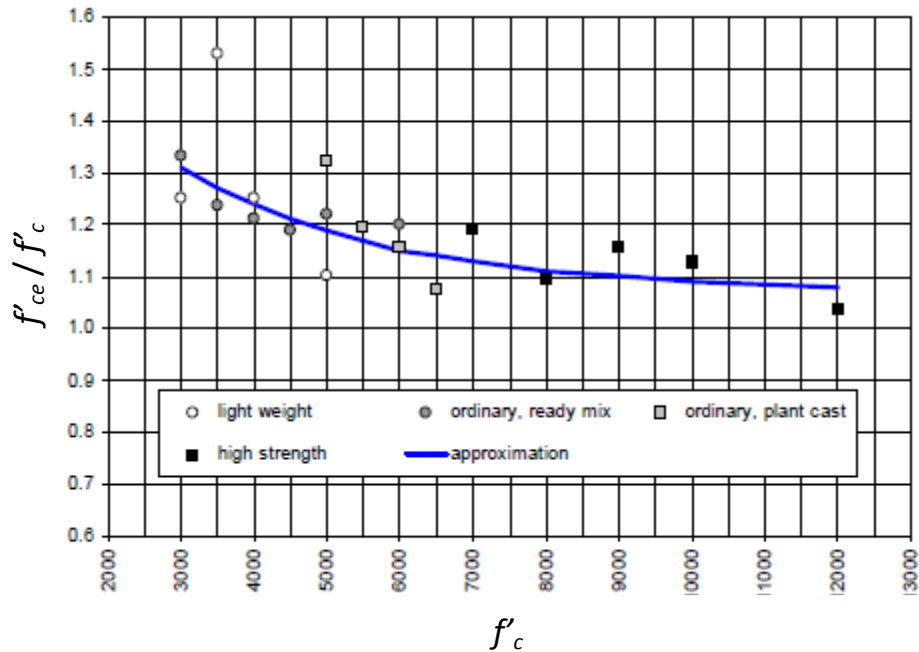


Figure 2.1. Expected Compressive Strength of Concrete
(Nowak et al, 2008)

C2.1.3

The use of $f'_{ce} = 1.3f'_c$, as permitted in LATBSDC (2014) and PEER TBI (2010), is not recommended, as a review of test results summarized in Nowak et al (2008) (Table 2.1 and Figure 2.1) indicates that this expression overestimates f'_{ce} , particularly for high strength concrete. Although regional differences exist in concrete materials (e.g., aggregate), which affects the ratio of f'_{ce} to f'_c , the recommended values provided in Table 2.1 and Figure 2.1 are intended to represent average values, and the use of a larger value for f'_{ce} is only permitted if it can be demonstrated to be reliable based on project-specific material test information.

2.2 Flexural Strength

2.2.1

The nominal plastic flexural strength, M_p , of an SRC coupling beam shall be computed using a plastic section analysis with the minimum specified yield strength of structural steel, F_y , as the plastic steel stress and the specified compressive strength of concrete, f'_c , used with a uniform magnitude (Whitney) stress block for concrete in compression. The contribution of concrete in tension to moment strength shall be neglected, and an iterative approach may be used to determine the neutral axis depth, x , of the composite member. A sample calculation using the recommended approach is provided in Appendix A.

C2.2.1

M_p is used in the determination of M_n in Section 2.2.3 and also in the determination of the effective stiffness in Section 2.4.1.

2.2.2

The expected plastic flexural strength, M_{pe} , may be computed in the same manner as M_p in Section 2.2.1, except that expected material properties are used in place of specified material properties, i.e., the expected yield strength of structural steel, F_{ye} , is used in place of F_y , and the expected compressive strength of concrete, f'_{ce} , is used in place of f'_c . Computing M_{pe} in this manner is not recommended for cases in which auxiliary transfer bars and bearing plates are provided (see Section 2.6.3 for more details on auxiliary transfer bars and bearing plates).

C2.2.2

Section H5.5d and Section H4.5b(2)(1) of the 2010 AISC Seismic Provisions specify that the expected flexural strength of an SRC coupling beam be computed using either the plastic stress distribution (strain compatibility is violated, but the calculation yields a sufficiently accurate result) or the strain compatibility method (using appropriate R_y factors for the various elements of the steel cross-section, i.e., web, flanges, in either analytical method). No specific equation to compute M_{pe} is provided in the 2010 AISC Seismic Provisions (nor a sample calculation), and calibration to test results is not mentioned (including in the Commentary). Based on a review of test results (Motter et al, 2013), computing M_{pe} using a plastic analysis approach was found to provide a reasonable upper bound estimate of the strength of flexural-yielding SRC coupling beams, which is required for application of capacity design concepts. For cases in which auxiliary transfer bars and bearing plates are provided, computing M_{pe} in this manner is not recommended, as test results (Gong and Shahrooz, 2001b) indicate that SRC coupling beam flexural strength exceeds M_{pe} . However, as the test specimens of Gong and Shahrooz (2001b) were shear-yielding members, further testing is needed to develop recommendations for computing M_{pe} for SRC coupling beams with auxiliary transfer bars and bearing plates.

2.2.3

The nominal flexural strength, M_n , is the moment value developed at the beam-wall interface based on developing M_p at $L_e/3$ from the beam-wall interface, where L_e is the embedment length of the steel section into the wall measured from the beam-wall interface to the embedded end of the steel section and is computed using Section 2.5.1. Therefore, nominal flexural strength, M_n , is computed as (Figure 2.2):

$$M_n = \frac{M_p L}{L_{eff}} = \frac{M_p L}{\left(L + \frac{2L_e}{3} \right)} \quad (2.1)$$

where L_{eff} is the effective span length and L is the clear span.

C2.2.3

The computation of M_n is based on M_p , L , and L_{eff} . In the computation of L_{eff} , the term $2L_e/3$ represents the added flexibility due to the gapping between the embedded steel flange and the wall concrete in the embedment region. The concept of effective fixity at $L_e/3$ from the beam-wall interface is consistent with the recommendation made by Shahrooz et al (1993) and is discussed in the Commentary (Commentary H4.3) of the 2010 AISC Seismic Provisions.

Based on a review of test results (Motter et al, 2013), Equation (2.1) was determined to produce a computed nominal flexural strength that may be developed for flexure-controlled SRC coupling beams over the range of rotations typically expected for coupling beams (i.e., up to about 6% chord rotation per Motter et al, 2013).

2.2.4

The relationship between beam shear and end moments is based on a fixed-fixed beam with a clear span of length L , leading to the following equations (Figure 2.2):

$$V @ M_{pe} = \frac{2M_{pe}}{L} \quad (2.2)$$

$$V @ M_p = \frac{2M_p}{L} \quad (2.3)$$

$$V @ M_n = \frac{2M_n}{L} = \frac{2M_p}{L_{eff}} = \frac{2M_p}{\left(L + \frac{2L_e}{3}\right)} \quad (2.4)$$

C2.2.4

$V @ M_{pe}$ is used in Section 2.3.3 to determine $V_{ne,limit}$, which is the limiting shear strength of the SRC coupling beam and is used for capacity design purposes in this document.

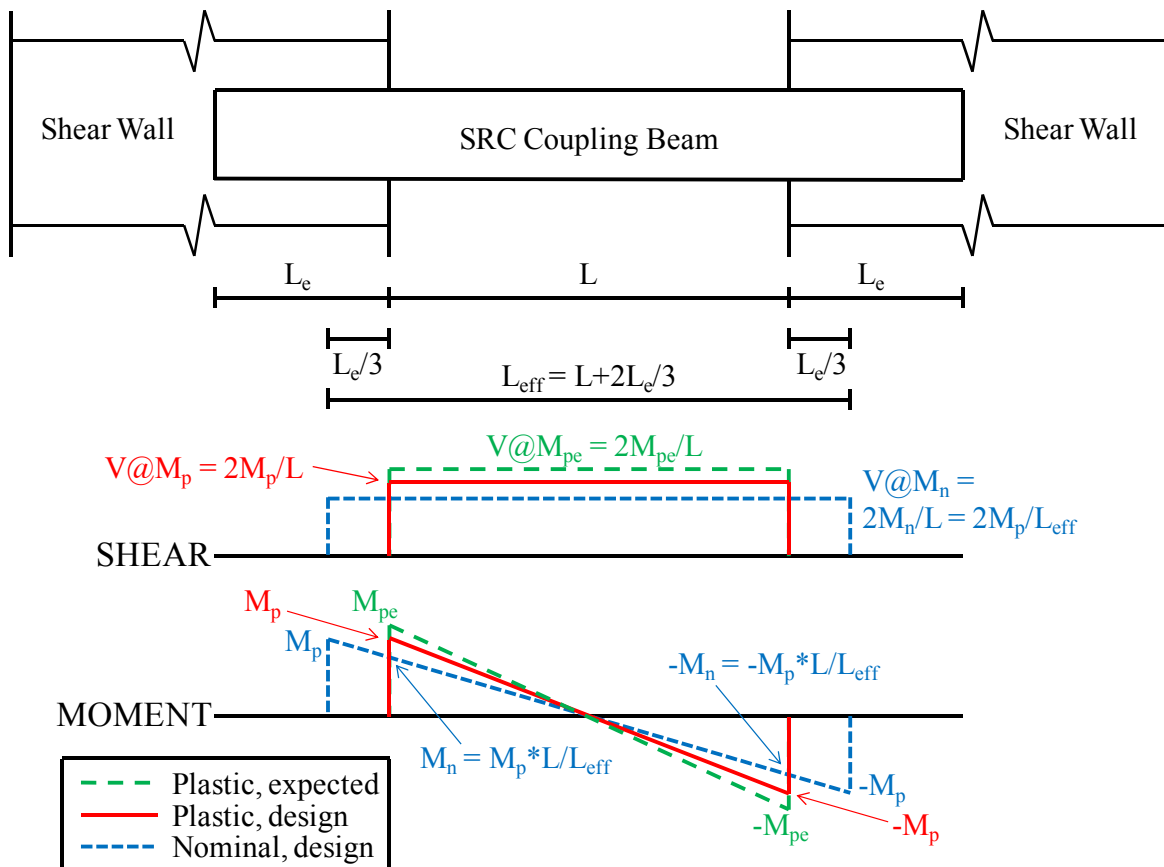


Figure 2.2. Flexural Capacities and Shear Demands

2.3 Shear Strength

2.3.1

The nominal shear strength, V_n , of an SRC coupling beam shall be computed as

$$V_n = V_p + 2\sqrt{f'_c}bd_c + \frac{A_{st}f_yd_c}{s} \quad (2.5)$$

where f'_c is the specified compressive strength of concrete, b is the beam width, i.e. the width of concrete encasement, d_c is the effective depth of concrete encasement, A_{st} is the area of transverse reinforcement, f_y is the specified yield strength of transverse reinforcement, s is the spacing of transverse reinforcement, and V_p is the nominal shear strength of the steel section, computed as $0.6F_yA_w$, where F_y is the specified minimum yield strength and A_w is the web area, taken as the product of the depth, d , and the web thickness, t_w .

C2.3.1

Based on a review of test results (Gong and Shahrooz, 2001b), Equation (2.5), which considers the contribution of structural steel, concrete, and transverse reinforcement to shear strength, was determined by Motter et al (2013) to produce a reasonable estimate of the nominal shear strength for SRC coupling beams over the range of rotations typically expected for coupling beams (i.e., up to about 6% chord rotation per Motter et al, 2013).

2.3.2

The expected shear strength, V_{ne} , of an SRC coupling beam shall be computed as:

$$V_{ne} = 1.1R_y V_p + 1.42 \left(2\sqrt{f'_{ce}} b d_c \right) + 1.33 \left(\frac{A_{st} f_{ye} d_c}{s} \right) \quad (2.6)$$

where R_y is the ratio of the expected to specified minimum yield strength of structural steel, f'_{ce} is the expected compressive strength of concrete, and f_{ye} is the expected yield strength of transverse reinforcement. Values for R_y , f_{ye} , and f'_{ce} shall be determined in accordance with Section 2.1. In Equation (2.6), f'_{ce} shall be input in units of psi to produce an output, $\sqrt{f'_{ce}}$, also in units of psi (a concept that is consistent with ACI 318-11).

C2.3.2

Equation (2.6) was derived by Motter et al (2013) from Equation H5-3 in the 2010 AISC Seismic Provisions, which is based on an equation developed by Gong and Shahrooz (2001b) by calibration with test results:

$$V_{ne} = 1.1R_y V_p + 1.56 \left(2\sqrt{f'_c} b d_c + \frac{A_{st} f_y d_c}{s} \right) \quad (2.7)$$

Equation (2.6) was modified from Equation (2.7) to be based entirely on expected material properties rather than specified material properties, since V_{ne} is an expected strength used for capacity design purposes, i.e., to determine the nominal strength of other components that are intended to remain elastic (e.g., the embedment strength, the strength of wall reinforcement crossing the embedment length). This approach is consistent with capacity design methods generally prescribed in building codes (e.g., ACI 318-11 for design of beam shear (Section

21.5.4.1) and joint shear (Section 21.7.2.1) for special moment frames). The modification of Equation (2.7) to produce Equation (2.6) is explained in the following paragraphs.

The coefficient for concrete shear strength was changed from 1.56 in Equation (2.7) to 1.42 in Equation (2.6) in order to remove concrete overstrength from the coefficient, and f'_c was changed to f'_{ce} to consider overstrength for a broader range of specified concrete compressive strengths than considered in the development of Equation (2.7). The 1.56 coefficient in Equation (2.7) was developed based on a parametric study that considered $f'_c = 4.0$ -ksi for 19 of the 24 cases analyzed and an average f'_c of 4.4-ksi (Gong and Shahrooz, 2001b). Therefore, a representative ratio of $f'_{ce} / f'_c = 1.21$ was obtained from Table 2.1 (Nowak et al, 2008) to develop Equation (2.6), i.e., $1.56 / \sqrt{1.21} = 1.42$. This modification was made to address the potential overprediction of V_{ne} for higher f'_c values, which are commonly used for high-rise construction. For example, for specified concrete compressive strength exceeding 6-ksi, the ratio f'_{ce} / f'_c is less than 1.21, and typically in the range of 1.1 to 1.2 (Table 2.1 and Figure 2.1, which correspond to Table 5-6 and Figure 5-7 in Nowak et al, 2008).

Similarly, the coefficient applied to the shear strength associated with shear reinforcement was modified from 1.56 in Equation (2.7) to 1.33 in Equation (2.6) to account for the reinforcement overstrength. Use of the ratio $f_{ye} / f_y = 1.17$ (which is based on the LATBSDC (2014) document and the PEER TBI (2010)) is consistent with Section 2.1.2, which led to a change in the coefficient from 1.56 to 1.33 ($1.56 / 1.17 = 1.33$). It should be noted that Nowak et al (2008) reported mean f_{ye} / f_y values of 1.18, 1.13, and 1.12 for #3, #4, and #5 Grade 60 reinforcement, respectively, indicating that it might be appropriate to use a slightly lower overstrength ratio for

smaller bar sizes commonly used for shear reinforcement. However, this refinement does not result in significant variation of V_{ne} and, thus, was not adopted here.

V_{ne} is used in Section 2.3.3 to determine $V_{ne,limit}$, which is the limiting shear strength of the SRC coupling beam and is used for capacity design purposes in this document.

2.3.3

The limiting shear strength, $V_{ne,limit}$, of an SRC coupling beam, to be used for capacity design purposes, shall be taken as the smaller of $V@M_{pe}$ (Section 2.2.4, Equation (2.2)) and V_{ne} (Section 2.3.2, Equation (2.6)).

C2.3.3

The limiting shear strength represents the expected shear force that the SRC coupling beam will develop, considering both expected shear strength and expected flexural strength of the beam. In this document, $V_{ne,limit}$ is used in Section 2.5.1 to determine the required embedment length and in Section 2.6.1.1 to determine the required strength of wall longitudinal reinforcement crossing the embedment length. This approach is consistent with capacity design methods generally prescribed in building codes (e.g., ACI 318-11 for design of beam shear (Section 21.5.4.1) and joint shear (Section 21.7.2.1) for special moment frames).

2.4 Effective Stiffness

2.4.1

Four approaches may be used to model the effective stiffness of flexure-controlled SRC coupling beams with $2 \leq (\alpha = L/h) \leq 4$ (where α is the span-to-depth ratio, i.e., the ratio of the clear span, L , to the overall beam height including concrete encasement, h) (Table 2.2), noting that the recommended stiffness values shall be reduced by 20% when checking lateral drift limits:

2.4.1.1

Beam effective stiffness is modeled using a rigid beam (for flexure and shear) with span length L along with rotational springs at the beam-wall interfaces with stiffness:

$$K = \frac{M_p}{\theta_y} \quad (2.8)$$

where K is the rotational spring stiffness, M_p is the nominal plastic flexural strength and θ_y is the coupling beam chord rotation at yield. Based on test results, θ_y may be estimated as 0.0133 radians (1.33%); therefore, $K = 75M_p/\text{radian}$ or $0.75M_p/(\% \text{ chord rotation})$.

2.4.1.2

Beam effective stiffness is modeled using an equivalent effective shear stiffness, $(EA)_{eff}$, along with a rigid flexural stiffness:

$$(EA)_{eff} = \frac{2K}{L} = \frac{2M_p}{\theta_y L} \quad (2.9)$$

2.4.1.3

Beam effective stiffness is modeled using an equivalent effective flexural stiffness, $(EI)_{eff}$, along with a rigid shear stiffness:

$$(EI)_{eff} = \frac{KL}{6} = \frac{M_p L}{6\theta_y} \quad (2.10)$$

2.4.1.4

Beam effective stiffness is modeled using an equivalent effective flexural stiffness, $(EI)_{eff}$, along with a rigid shear stiffness:

$$(EI)_{eff} = 0.06\alpha E_s I_{trans} \quad (2.11)$$

where E_s is the modulus of elasticity of steel, and I_{trans} is the moment of inertia of the transformed section (concrete transformed to steel based on the modular ratio, with the modulus of elasticity of concrete, E_c , based on ACI 318-11 Section 8.5.1) neglecting cracked concrete (i.e., not considering concrete tensile strength).

Table 2.2: *Stiffness Modeling Approaches for Flexure-Controlled Beams with $2 \leq (\alpha = L/h) \leq 4$*

Stiffness Modeling Approach	Interface Slip/Extension Spring Stiffness	Effective Shear Stiffness	Effective Bending Stiffness
(1)	Equation (2.8)	Rigid	Rigid
(2)	Rigid	Equation (2.9)	Rigid
(3)	Rigid	Rigid	Equation (2.10)
(4)	Rigid	Rigid	Equation (2.11)

C2.4.1

The recommended stiffness values are based on tests of flexure-yielding specimens with aspect ratios of 3.33 and 2.4 (Motter et al, 2013). Modest extrapolation of test results to include flexure-yielding SRC coupling beams between aspect ratios of two and four is recommended. Reducing effective stiffness values by 20% when checking lateral drift limits reflects uncertainty in the measured stiffness values (see Motter et al, 2013, for more details).

Equation (2.8) is based on test results reported by Motter et al (2013), which indicate that slip and extension (or pullout) of the steel section from the embedment region (at the beam-wall interface) was the primary source of coupling beam chord rotation, while the relative contributions of shear and flexure deformations to the overall deformations were small. It is noted that this finding is consistent with recent test results for diagonally-reinforced and conventionally-reinforced coupling beams reported by Naish et al (2013a,b).

Although Equation (2.8) reasonably captures test results (Motter et al, 2013), designers are accustomed to modeling coupling beam stiffness as either shear stiffness and/or bending stiffness. Therefore, the spring stiffness of Equation (2.8) is converted into an equivalent shear

stiffness (Equation (2.9)) or bending stiffness (Equation (2.10)). Equation (2.11), is an alternative to Equation (2.10), but is based on using a transformed section. It is noted that, for simplicity, all four approaches lump beam flexibility into a single modeling parameter. Given the relatively sparse test results at this time, use of a more complicated modeling approach does not appear justified.

Sections H4.3 and H5.3 of the 2010 AISC Seismic Provisions refer to ACI 318 Chapter 10 for the determination of the effective bending stiffness of SRC coupling beams for elastic analysis and note that shear deformations and connection flexibility should also be considered (but provide limited details as to how this shall be accomplished). ACI 318-11 Section 10.10.4.1 specifies an effective moment of inertia of $0.35I_{g,c}$ for beams, where $I_{g,c}$ is the moment of inertia of the gross concrete section neglecting the impact of reinforcement (a transformed section analysis is not required). Use of the ACI 318 Chapter 10 provisions is not recommended, as the expressions developed in this section provide more guidance and were developed based on test data.

2.4.2

The 2010 AISC Seismic Provisions, in Commentary H4.3, provide an alternative expression to compute the effective moment of inertia, I_{eff} , for either steel or SRC coupling beams of any aspect ratio:

$$I_{eff} = 0.60I_{g,s} \left(1 + \frac{\lambda 12 E_s I_{g,s}}{L_c^2 G_s A_w} \right)^{-1} = 0.60kI_{g,s} \quad (2.12)$$

where k represents the reduction in flexural stiffness due to shear deformations, $I_{g,s}$ is the moment of inertia of the gross steel section (neglecting reinforced concrete encasement, where applicable), E_s is the modulus of elasticity of steel, G_s is the shear modulus of steel, A_w is the area of the steel section resisting shear (taken as the product of the steel section depth, d , and web thickness, t_w), λ is the cross-section shape factor for shear (1.5 for W-shapes), and L_c is the effective clear span of the coupling beam, computed as $L_c = L + 2c$ to account for spalling of the wall clear cover, c . Given that I_{eff} per Equation (2.12) is reduced to account for shear deformations using k , the beam shear stiffness should be modeled as rigid, unless shear deformations are modeled separately, in which case $k = 1$. When using $k = 1$, modeling an effective shear stiffness of $0.6G_sA_w/\lambda$ is consistent with Equation (2.12).

C2.4.2

Equation (2.12), which considers both flexural and shear deformations, is based on tests of steel coupling beams without concrete encasement (Harries et al, 1993, and Harries et al, 1997). It is noted that the exponent (-1) was erroneously omitted in the expression provided in the Commentary of the 2010 AISC Seismic Provisions but is included in Equation (2.12) to be consistent with Harries (1995) and Harries et al (2000).

The effective coupling beam stiffness is identical when using Equation (6.8), Equation (6.9), or Equation (6.10) in Section 2.4.1. From the statistical data shown in Table 2.3, which are based on a parametric study by Motter et al (2013) for 48 variations of beam cross-section, beam span-to-depth (aspect) ratio, and concrete compressive strength, it is evident that there is minimal difference in stiffness values obtained with Equation (6.10) and Equation (6.11) and

modest difference in stiffness values obtained with Equation (6.12) and either Equation (6.10) or Equation (6.11). On average (i.e., using the statistical results in Table 2.3), relative to the effective stiffness obtained using Equation (2.10), the effective stiffness obtained using Equation (2.11) is roughly 10% larger with a coefficient of variation of 3%, whereas the effective stiffness obtained using Equation (2.12) is roughly 20% larger with a coefficient of variation of roughly 15% (Table 2.3). The sensitivity of differences between stiffness values computed using Equation (2.12) and either Equation (2.10) or Equation (2.11) is due in part to the treatment of concrete encasement, noting that concrete encasement is not considered in Equation (2.12) but is considered in Equation (2.10) and Equation (2.11).

Table 2.3: *Statistical Summary of Results of Parametric Study on Stiffness*

	$I_{eff} / I_{g,s}$			Eq. (2.11) / Eq. (2.10)	Eq.(2.12) / Eq. (2.10)	Eq. (2.12) / Eq. (2.11)
	Eq. (2.12)	Eq. (2.10)	Eq. (2.11)			
Minimum	0.12	0.13	0.14	1.05	0.89	0.80
Maximum	0.47	0.39	0.44	1.17	1.66	1.48
Mean	0.29	0.24	0.26	1.11	1.19	1.08
Standard Deviation	0.10	0.08	0.08	0.04	0.17	0.16
Coefficient of Variation	0.35	0.32	0.32	0.03	0.14	0.15

2.5 Embedment Length

2.5.1

The embedment strength, $V_{n,embed}$, which is the peak beam shear load that the embedment can resist, is computed as (Equation H4-2 in the 2010 AISC Seismic Provisions):

$$V_{n,embed} = 1.54 \sqrt{f'_c} \left(\frac{b_w}{b_f} \right)^{0.66} \beta_1 b_f (L_e - c) \left[\frac{0.58 - 0.22\beta_1}{0.88 + \frac{L + 2c}{2(L_e - c)}} \right] \quad (2.13)$$

where b_w is the wall thickness, b_f is the beam flange width, L_e is the provided embedment length of the steel section into the reinforced concrete structural wall (measured from the beam-wall interface), L is the beam clear span, c is the wall clear cover measured from the edge of the wall to the outside of the transverse boundary reinforcement if a boundary element is present or to the outside of the outermost longitudinal reinforcement if a boundary element is not present, and β_1 is the depth factor, relating the depth of the equivalent uniform magnitude (Whitney) stress block to the neutral axis depth, x . Providing $V_{n,embed} \geq V_{ne,limit}$ (with $V_{ne,limit}$ defined in Section 2.3) is recommended, with $V_{n,embed} = V_{ne,limit}$ used to solve for the minimum required L_e in Equation (2.13). Note that f'_c , which is input in units of ksi to produce an output, $\sqrt{f'_c}$, in units of ksi, is used rather than f'_{ce} in Equation (2.13).

C2.5.1

Equation (2.13), which is Equation H4-2 in the 2010 AISC Seismic Provisions, is consistent with the Mattock and Gaafar (1982) embedment equation, modified to account for concrete

spalling at the beam-wall interface per the recommendation of Harries et al (1993). A strength reduction factor of 0.9 is inherent in Equation (2.13) relative to the Mattock and Gaafar (1982) embedment equation. The definition of c is consistent with that provided in the 2010 AISC Seismic Provisions Commentary H4.5b. Determining the minimum required embedment length by taking $V_{n,embed} = V_{ne,limit}$, where $V_{ne,limit}$ is the lesser of V_{ne} and $V@M_{pe}$, in Equation (2.13) is consistent with Section H5.5d and H4.5b(2)(1) of the 2010 AISC Seismic Provisions.

Equation (2.13) is consistent with the embedment model shown in Figure 2.3, originally developed by Marcakis and Mitchell (1980) and Mattock and Gaafar (1982) and modified to account for spalling by Harries et al (1993). Equation (2.13) is based on satisfying force and moment equilibrium due to the development of concrete bearing stresses/forces acting normal to the flanges along the length of the embedded steel section and $V_{n,embed}$ applied at a cantilever distance, a from the beam-wall interface. Both models assume a linear concrete strain distribution in the embedment region with a strain of 0.003 at the outer face, from which a uniform magnitude (Whitney) stress block is assumed along the front portion of the embedded member. The ACI stress block factor, β_1 , is used to relate the depth of the Whitney stress block to the neutral axis depth, x . The Hognestad (1955) parabolic stress-strain relationship is used to determine the stress distribution along the back portion of the embedded member (since the strain at the back end of the embedded member is not 0.003, negating the use of a Whitney stress block), where ε_0 is the strain corresponding to the specified compressive strength of concrete, f'_c , and is typically taken as 0.002, and f_c is the concrete stress computed at the strain of interest, ε_c . C_f and C_b are the resultant concrete bearing forces that develop at the front and back, respectively, of the embedded steel section.

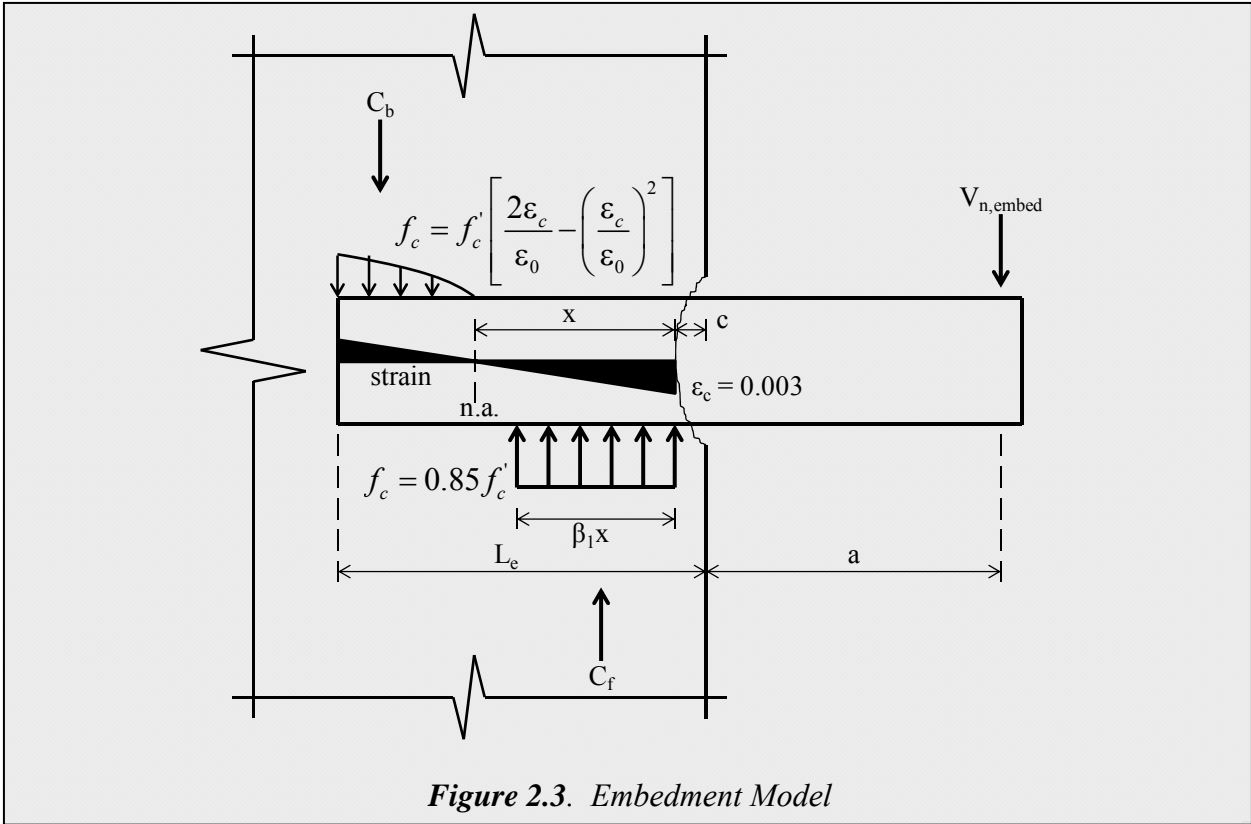


Figure 2.3. Embedment Model

2.6 Embedment Detailing

2.6.1 Wall Longitudinal Reinforcement

2.6.1.1

Wall longitudinal reinforcement crossing normal to the embedment length of the structural steel member into the wall should satisfy:

$$A_s f_y \geq C_b = \left(\frac{\frac{(L + 2c)}{2(L_e - c)} + 0.33\beta_1}{0.88 - 0.33\beta_1} \right) V_{ne,limit} \quad (2.14)$$

where C_b is the resultant concrete bearing force developed within the embedment zone, located near the back of the embedded steel section and acting normal to the flange of the embedded steel section (Figure 2.3). The value of L_e in Equation (2.14) shall not be taken greater than 1.25 times the minimum required embedment length computed using $V_{n,embed} = V_{ne,limit}$ in Equation (2.13) in Section 2.5.1, even if the provided embedment length exceeds the minimum required embedment length by a factor larger than 1.25. Wall longitudinal reinforcement required by Equation (2.14) shall extend at least one development length for f_y in tension above the top flange and below the bottom flange of the structural steel beam.

C2.6.1.1

The quantity of wall longitudinal reinforcement required by Equation (2.14) is typically more than that required by Section H4.5b(1)(4) of the 2010 AISC Seismic Provisions, where

$A_s f_y \geq V_{ne,limit}$ must be provided over the embedment length of the beam, with at least two-thirds of the steel provided between the beam-wall interface and one-half of the embedment length ($L_e/2$). At upper-level stories of coupled walls, satisfying Equation (2.14) may require more wall boundary longitudinal reinforcement than is required to resist design actions (P_u and M_u).

Equation (2.14) was developed by Motter et al (2013) based on an examination of load paths within the embedment region of the wall using strut-and-tie (truss) models. Use of a strut-and-tie model indicates that the coupling beam bearing forces (C_f and C_b in Figure 2.3) create a local increase in the force on the wall longitudinal reinforcement in the vicinity of the embedded steel section. This local increase is proportional to the back bearing force (which is the smaller of the two bearing forces), C_b , rather than $V_{ne,limit}$. The added local tensile demand can lead to yielding of boundary longitudinal reinforcement when global demands are not large enough to produce yielding. Test results reported by Motter et al (2013) indicate that failure to satisfy Equation (2.14) contributes to local yielding of wall boundary longitudinal reinforcement and associated damage in the embedment region, which leads to lower SRC beam strength in addition to significant pinching of the beam force-deformation behavior (e.g., shear force vs. chord rotation). The tests by Motter et al (2013) also indicate that adequate performance can be achieved without requiring at least two-thirds of the vertical wall reinforcement crossing the embedment length to be located between the beam-wall interface and one-half of the embedment length.

In Equation (2.14), increasing the provided embedment length decreases C_b and the required $A_s f_y$. Although longer embedment length is associated with better performance, providing additional embedment length well in excess of the required embedment length is unlikely to improve performance. Therefore, a limit was placed on the maximum value that may be used for L_e in Equation (2.14).

The 2010 AISC Seismic Provisions require that wall longitudinal reinforcement used to provide $A_s f_y$ extend at least one development length for f_y in tension above the top flange and below the bottom flange of the structural steel beam. The intent of this requirement is to ensure that the reinforcement may develop the yield force beyond the critical sections, located at the bearing surfaces between structural steel and the surrounding concrete. It is noted that satisfying this recommendation may influence the location of bar cut-offs.

A parametric study conducted by Motter et al (2013), which considered 48 variations of beam cross-section, beam span-to-depth (aspect) ratio, and concrete compressive strength, was used to assess the difference in wall longitudinal reinforcement required by Equation (2.14) ($A_s f_y \geq C_b$) and that required by AISC ($A_s f_y \geq V_{ne,limit}$). The parameter $M@V_{ne,limit}$, which is the moment at the beam-wall interface corresponding to the development of $V_{ne,limit}$, was of interest in this parametric study, as this parameter is a better indicator of the strength of flexure-controlled sections than $V_{ne,limit}$. A summary of the results of the parametric study (Table 2.6) indicates (based on comparing the ratio of $C_b / V_{ne,limit}$) that Equation (2.14) requires more longitudinal reinforcement on average than that required by AISC, noting that the difference increases with increasing aspect ratio. Because most of the beams considered in formulating Table 2.6 are

flexure-controlled, the ratio $C_b / V_{ne,limit}$ increases with increasing aspect ratio, while the ratio $M@V_{ne,limit} / C_b$ is nearly constant. This nearly-constant relationship between C_b and $M@V_{ne,limit}$ suggests that using C_b rather than $V_{ne,limit}$ to determine the required strength of wall longitudinal reinforcement crossing the embedment length is appropriate for flexure-controlled beams, which are controlled by $M@V_{ne,limit}$ rather than $V_{ne,limit}$.

Table 2.6: *Statistical Summary of Results of Parametric Study on Wall Longitudinal Reinforcement*

Aspect Ratio, α	$C_b / V_{ne,limit}$					$C_b / M@V_{ne,limit} (ft^{-1})$				
	Min.	Max.	Mean	Standard Deviation	Coefficient of Variation	Min.	Max.	Mean	Standard Deviation	Coefficient of Variation
1.75	0.94	1.29	1.08	0.11	0.10	0.39	0.84	0.57	0.13	0.23
2.40	1.16	1.74	1.40	0.18	0.13	0.35	0.81	0.54	0.15	0.27
3.33	1.63	2.41	1.95	0.25	0.13	0.36	0.81	0.54	0.15	0.27
4.00	1.98	2.90	2.36	0.30	0.13	0.36	0.81	0.55	0.15	0.27

The tests reported by Motter et al (2013), which were the basis for the development of Equation (2.14), considered a more critical wall-loading condition (i.e. with cyclic wall loading) than the tests of Harries et al (1993) and Harries et al (1997), which were the basis for the development of the AISC equation. Harries (1995) developed the recommendation for $A_s f_y \geq V_{ne,limit}$ based on the results of four laboratory tests (Harries et al, 1993, and Harries et al, 1997) conducted on steel coupling beams (without concrete encasement) embedded into wall segments that were post-tensioned to loading beams. The post-tensioning of the wall segments created compression normal to the length of the embedded steel section, improving load-transfer between the beam and the wall. The test set-up used by Motter et al (2014) included the application of reversed-cyclic loading to a wall panel with embedded SRC beams. This loading

approach created alternating (cyclic) tension and compression normal to the embedment length. Because the transfer of coupling beam bearing forces into wall reinforcement creates local tensile demands, the more critical loading condition occurs when the wall demands create tension normal to the connection. As the tests conducted by Harries et al (1993) and Harries et al (1997) did not include a cyclically-loaded wall, the development of the $A_s f_y > V_{ne,limit}$ recommendation was based on tests that did not consider this critical load-transfer condition. The test results reported by Motter et al (2013) (specifically SRC3, for which Equation (2.14) is not satisfied but the AISC provision is satisfied) indicate that failure to satisfy Equation (2.14) will lead to greater pinching and cyclic degradation in load-deformation response of the coupling beam than may be implied by the R-factor used for design of the lateral force-resisting system.

2.6.2 Wall Boundary Transverse Reinforcement

2.6.2.1

Wall boundary transverse reinforcement (hoops and ties) within the embedment region shall be required based on ACI 318-11 Section 21.9.6.4 (as required by Section 21.9.6.2 or Section 21.9.6.3) or Section 21.9.6.5 with slight modification to Section 21.9.6.5 as follows: Within the embedment region, extending at least one coupling beam embedment length (L_e) above the top flange and below the bottom flange of the embedded steel section, it is recommended that the detailing requirements of Section 21.9.6.5(a) be satisfied as if $\rho > 400/f_y$, for cases in which $\rho \leq 400/f_y$.

C2.6.2.1

For taller buildings that utilize Special Structural Walls, boundary transverse reinforcement satisfying ACI 318-11 Section 21.9.6.4, the well-detailed region of the wall, is typically provided only near the wall base where moment and axial load demands on the wall tend to produce the highest stresses and strains. Above this region, wall boundary transverse reinforcement need only satisfy ACI 318-11 Section 21.9.6.5. Per Section 21.9.6.5, if the wall boundary longitudinal reinforcement ratio, $\rho > 400/f_y$, where f_y is the specified yield strength of this reinforcement in units of psi, then modest detailing must be provided with vertical spacing of hoops and crossties limited to a maximum of 8" (200 mm) on center. For ACI 318-14, Section 18.10.6.5, the 8" limit will be modified to be the smaller of 8" and $8d_b$, except at yielding sections above the well-detailed (plastic hinge) region near the wall base, where the limit will be reduced to 6" and $6d_b$. It is recommended that these new limits be satisfied.

Where the wall boundary longitudinal reinforcement ratio, $\rho \leq 400/f_y$, hoops and crossties need not be provided, and horizontal web reinforcement is typically lapped with U-bars at the wall boundary (ACI 318-11 Section 21.9.6.5). However, until further testing indicates that doing so is unnecessary, providing hoops and cross-ties in the embedment region is recommended for all SRC coupling beams (even for cases in which $\rho \leq 400/f_y$). Extending this wall boundary transverse reinforcement at least L_e above the top flange and below the bottom flange of the embedded steel section provides restraint against buckling of wall longitudinal reinforcement over the region susceptible to localized demands from coupling beam bearing forces. Therefore, wall boundary longitudinal reinforcement may need to extend beyond the distance required in Section 2.6.1.1 (i.e., one development length for f_y in tension above the top flange and below the bottom flange of the structural steel beam). For constructability, extending the wall boundary transverse reinforcement over the full story height where SRC coupling beams are used is suggested.

2.6.2.2

Due to the difficulty associated with passing hoops and ties through the web of the embedded steel section, it is permissible to use the detail shown in Figure 2.4, in which holes are pre-drilled through the web of the steel section to allow the use of threaded rods and steel plates to provide an equivalent $A_s f_y$ and spacing of transverse reinforcement through the embedment region (for the specified yield strength values of the plate and rods). It is also permissible to use the detail shown in Figure 2.5, in which holes are pre-drilled through the flanges of the steel section to allow the use of short-length threaded rods (spanning vertically between the flanges) with conventional rebar hoops and cross-ties. Alternative approaches to that shown in Figure 2.4 are

acceptable if they provide concrete confinement and restraint against rebar buckling that is equivalent to, or better than, that provided by conventional rebar hoops and cross-ties.

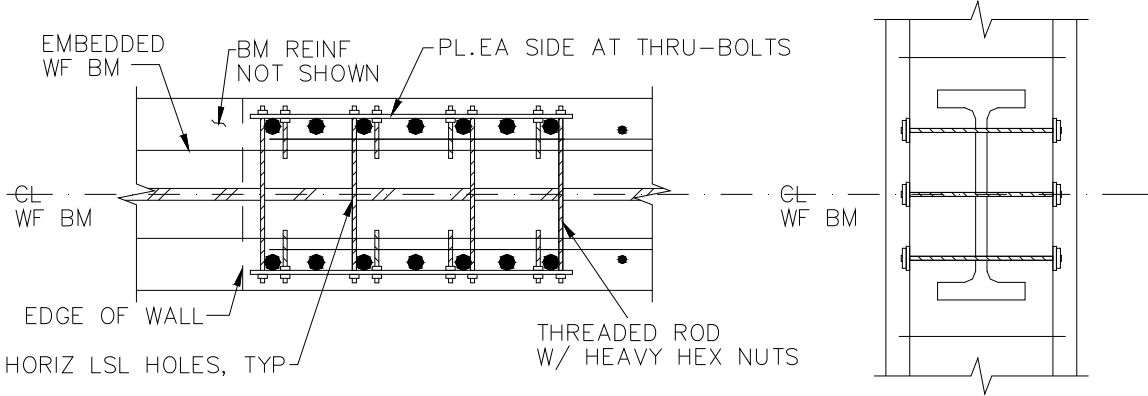


Figure 2.4. Threaded Rods and Side Plates at Embedded Steel Section

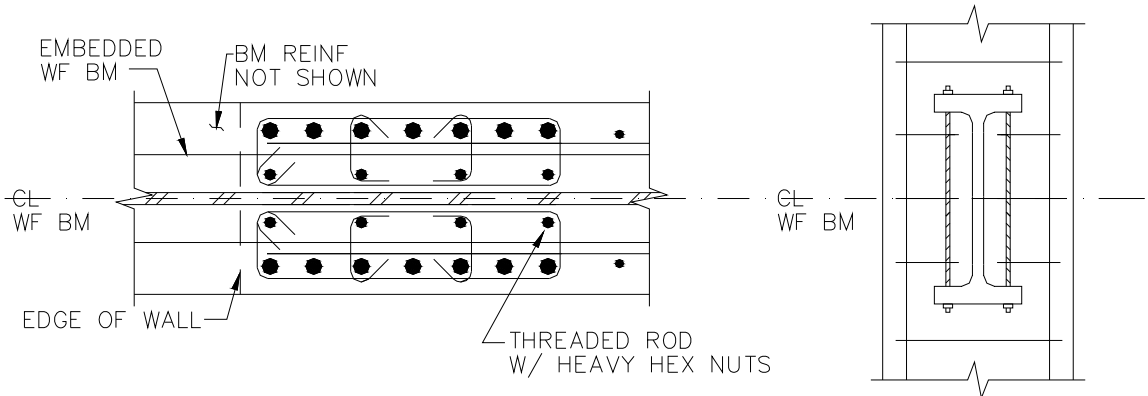


Figure 2.5. Threaded Rods and Conventional Hoops and Ties at Embedded Steel Section

C2.6.2.2

The use of conventional wall boundary transverse reinforcement at the location of an embedded steel section is not practical due to the construction-related difficulties associated with passing hoops and cross-ties (with seismic hooks) through the web of the steel section. However, it is necessary to provide wall boundary transverse reinforcement over the height of the embedded steel section per Section 2.6.2.1. The details shown in Figure 2.4 and Figure 2.5 are an

improvement upon the detail used in the tests conducted by Motter et al (2013), noting that the detail used by Motter et al (2013) provided adequate performance consistent with the recommendations provided. Further improvement to the embedment detail shown in Figure 2.4 might be accomplished by restraining every wall boundary longitudinal bar against buckling and/or including side plates along the inside of the wall boundary longitudinal bars to improve the stability of the short-length threaded rods (Figure 2.6).

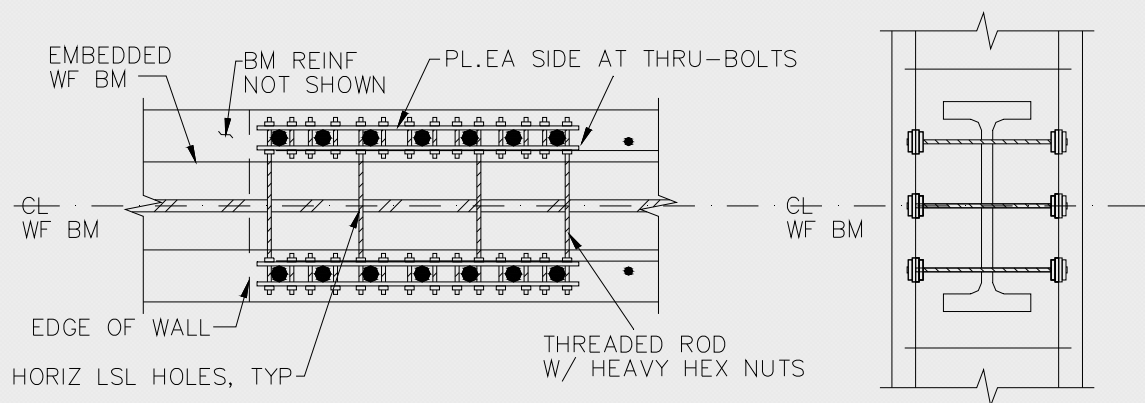


Figure 2.6. *Threaded Rods and Side Plates at Embedded Steel Section Providing Improved Restraint Against Bar Buckling*

At wall boundary locations where horizontal web reinforcement is required to be provided with either 90-degree hooks or spliced to U-bars per ACI 318-11 Section 21.9.6.5(b), due to the difficulty associated with passing 90-degree hooks or U-bars through the web of the embedded steel section, an alternative detail (Figure 2.7), where individual U-bars spliced to individual horizontal web bars in the embedment region (without passing the U-bar through the web of the steel section), was used in the tests conducted by Motter et al (2013).

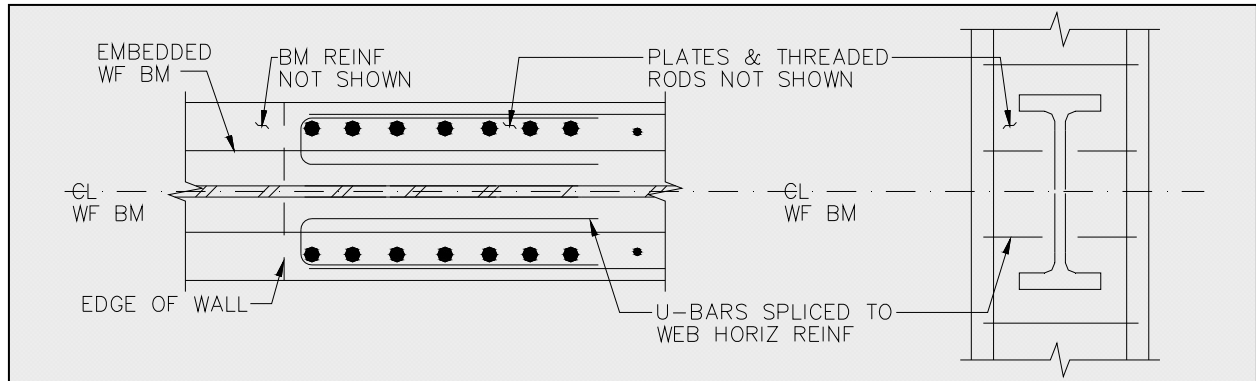


Figure 2.7. *U-Bars Spliced to Horizontal Web Reinforcement at Embedded Steel Section*

2.6.3 Auxiliary Transfer Bars and Bearing Plates

2.6.3.1

Auxiliary transfer bars and bearing plates (Figure 2.8), as required by the 2010 AISC Seismic Provisions, are not required.

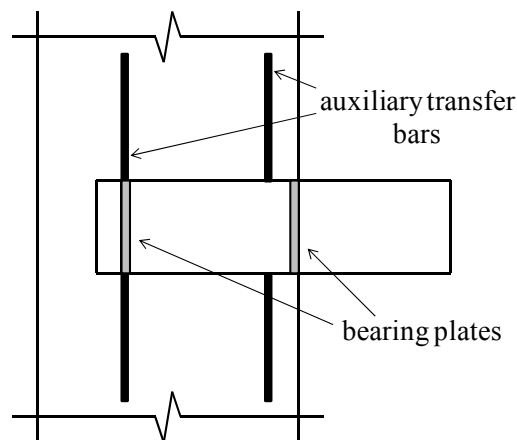


Figure 2.8. Auxiliary Transfer Bars and Bearing Plates per 2010 AISC Seismic Provisions

C2.6.3.1

The 2010 AISC Seismic Provisions (Section H5.5d for SRC coupling beams, which references provisions in Section H5.5c for steel coupling beams) require the use of auxiliary transfer bars attached to both the top and bottom flange of the embedded steel section, at both the front and back of the embedment zone, and bearing plates at the location of the back transfer bars and at the beam-wall interface (Figure 2.8). The use of the auxiliary transfer bars and bearing plates has been shown to improve the performance of SRC coupling beams, i.e., increasing strength modestly and reducing the degree of pinching that occurs in the load-deformation response (Shahrooz et al, 1993). However, test results reported by Motter et al (2013) indicate that the use of auxiliary transfer bars and bearing plates complicates construction and is not necessary

when providing adequate embedment length (Section 2.5.1), sufficient wall boundary vertical reinforcement (Section 2.6.1) and adequate wall boundary transverse reinforcement (Section 2.6.2). The recommendations for flexural strength (Section 2.2) were developed for SRC coupling beams without transfer bars and bearing plates. Recommendations for computing the expected plastic flexural strength, M_{pe} , in Section 2.2.2 are not applicable if auxiliary transfer bars and bearing plates are used (see C2.2.2 for more details).

2.7 Concrete Encasement Detailing

2.7.1

Longitudinal and transverse reinforcement shall be distributed around the beam perimeter with total area in each direction not less than $0.002bs$ and center-to-center spacing, s , not exceeding 12”.

C2.7.1

ACI 318-11 Section 21.9.7.4 describes two confinement options for diagonally-reinforced concrete coupling beams. One option is to provide transverse reinforcement enclosing each group of diagonal bars (Section 21.9.7.4(c)), and the other option is to provide transverse reinforcement for the entire beam cross-section (Section 21.9.7.4(d)). For the first confinement option, ACI 318-11 Section 21.9.7.4(c) requires that longitudinal and transverse reinforcement be distributed around the beam perimeter with total area in each direction not less than $0.002bs$ and spacing, s , not exceeding 12”. Satisfying this requirement, which typically requires providing more than the minimum shear reinforcement required by ACI 318-11 Section 11.4.6.3, is recommended for SRC coupling beams in order to be consistent with code provisions for diagonally-reinforced coupling beams. Referring to ACI 318-11 Figure R21.9.7(a), the confined diagonal bars are essentially replaced with a steel section for SRC coupling beams without altering the detailing around the perimeter of the beam.

2.7.2

Each beam longitudinal bar shall be of equal or larger diameter relative to the bar diameter of the transverse reinforcement.

C2.7.2

ACI 318-11 Section 21.9.7.4(d) requires that each beam longitudinal bar be of equal or larger diameter relative to the bar diameter of the transverse reinforcement. Satisfying this requirement for SRC coupling beams maintains consistency between detailing requirements for diagonally-reinforced and steel-reinforced concrete coupling beams.

2.7.3

Developing beam longitudinal reinforcement into the wall is not recommended. The extension of the beam longitudinal reinforcement into the wall shall be limited to 6”.

C2.7.3

Developing beam longitudinal reinforcement into the wall is not recommended for diagonally-reinforced concrete coupling beams per ACI 318-11 Figure R21.9.7(a). Adhering to this recommendation for SRC coupling beams avoids increasing M_{pe} . Although extension of beam longitudinal reinforcement into the wall avoids discontinuity at the beam-wall interface, limiting this extension to 6” ensures that beam longitudinal reinforcement will not be developed.

3. ALTERNATIVE (NON-PRESCRIPTIVE) DESIGN GUIDELINES

In this document, it is assumed that alternative (non-prescriptive) analysis procedures are accomplished using both linear response spectrum analysis (e.g., for service and wind level earthquake shaking and design level earthquake shaking) and nonlinear response history analysis (e.g., for maximum considered earthquake (MCE) level shaking), which is consistent with existing consensus documents for alternative design procedures for tall buildings, such as the Los Angeles Tall Buildings Structural Design Council document (LATBSDC, 2014), the Structural Engineers Association of Northern California (SEAONC) AB-083 Tall Buildings Task Group Recommended Administrative Bulletin for San Francisco (SEAONC AB-083, 2007), and the Pacific Earthquake Engineering Research (PEER) Center Tall Buildings Initiative (PEER TBI, 2010). The recommendations provided in this section are intended to be used in conjunction with these existing consensus documents.

Guidance and recommendations are provided in the following subsections: (3.1) applicability of prescriptive recommendations (for alternative analysis), (3.2) modeling and behavior categories, and (3.3) wall demands. These guidelines and recommendations were developed based on a review of test results and existing literature, as well as the recommendations for prescriptive design in Section 2 of this document. The primary test results used as the basis for developing these alternative (non-prescriptive) recommendations are the four flexure-yielding (aspect ratios of 2.4 and 3.33) SRC coupling beams, which did not include auxiliary transfer bars or bearing plates, reported by Motter et al (2013).

3.1 Applicability of Prescriptive Design Guidelines

The recommendations for prescriptive-based design (Section 2) shall be followed for alternative design, with the following modifications:

3.1.1

Expected Material Properties (Section 2.1): No modification. It is noted that expected material properties should be used for all calculations used in alternative analysis (i.e., for all calculations in Section 3).

C3.1.1

The use of expected material properties for all computations in Section 3 is consistent with alternative analysis approaches presented in consensus documents (LATBSDC, 2014; SEAONC AB-083, 2007; and PEER TBI, 2010).

3.1.2

Flexural Strength (Section 2.2): The computation of M_p , $V@M_p$, M_n , and $V@M_n$ is unnecessary.

C3.1.2

The computation of M_p , $V@M_p$, M_n , and $V@M_n$ is unnecessary for alternative analysis because modeling of the load-deformation response of flexure-controlled SRC coupling beams is matched to test data based on M_{pe} or $V@M_{pe}$ (Appendix B and Motter et al, 2013). Further explanation is provided in Section 3.2.

3.1.3

Shear Strength (Section 2.3): The computation of V_n is unnecessary.

C3.1.3

The computation of V_n is unnecessary for alternative analysis because modeling of the load-deformation response of shear-controlled SRC coupling beams should be matched to test data based on V_{ne} (Gong and Shahrooz, 2001a,b).

3.1.4

Effective Stiffness (Section 2.4): For design-level and MCE-level analysis, effective stiffness shall be determined in accordance with Section 2.4, except that M_{pe} shall be used in place of M_p , and E_c , which is used to determine I_{trans} , shall be computed using f'_{ce} rather than f'_c . Effective stiffness shall be increased by a factor of 1.5 for service-level analysis.

C3.1 4

Consistent with consensus design documents (LATBSDC, 2014; SEAONC AB-083, 2007; and PEER TBI, 2010), the determination of effective stiffness shall be based on expected material properties.

The LATBSDC (2014) document differentiates between reinforced concrete component stiffness values used for service- and wind-level loading versus values used for MCE-level loading. For reinforced concrete coupling beams, the effective bending stiffness for service- and wind-level loading is 1.5 times larger than that for MCE-level loading. The use of a larger

coupling beam effective stiffness value for service-level analysis requires greater member strengths to limit Demand-to-Capacity (D/C) ratios to acceptable values (typically 1.5). A similar approach is recommended, i.e., use of a service-level effective stiffness value for SRC coupling beams that is 1.5 times the value used for MCE-level design.

3.1.5

Embedment Length (Section 2.5): The expected compressive strength of concrete, f'_{ce} , shall be used in place of the specified compressive strength of concrete, f'_c , in Equation (2.13).

C3.1.5

Expected material properties are to be used for all computations in Section 3, including embedment strength. Because the embedment strength is dependent on the compressive strength of concrete, a reliable estimate of the embedment strength depends on an accurate estimate of f'_{ce} . Overestimating f'_{ce} corresponds to an overestimate of the embedment strength, which should be avoided in order to satisfy capacity design, i.e. to ensure that the embedment strength is larger than $V_{ne,limit}$.

3.1.6

Embedment Detailing (Section 2.6):

- Wall Longitudinal Reinforcement (Section 2.6.1): Equation (2.14) need not be satisfied, as the ratio of the expected strength of reinforcement crossing the embedment length, $A_s f_{ye}$, to the coupling beam back bearing force, C_b , is instead used to categorize the level of wall boundary reinforcement provided.

- Wall Boundary Transverse Reinforcement (Section 2.6.2): Section 2.6.2.1 shall be modified such that ACI 318-11 Section 21.9.6.5 shall be satisfied (when applicable) without modification (i.e., it is permissible to provide no wall boundary transverse reinforcement when $\rho \leq 400/f_y$).
- Auxiliary Transfer Bars and Bearing Plates (Section 2.6.3): No modification.

C3.1.6

The ratio of the expected strength of wall longitudinal reinforcement crossing the embedded steel section to the expected back bearing force, i.e., the ratio $A_s f_{ye} / C_b$, is used as a basis for categorizing the coupling beam force-deformation behavior, with categories of heavy ($A_s f_{ye} / C_b \geq 1.0$), modest ($0.5 \leq A_s f_{ye} / C_b < 1.0$), and light ($A_s f_{ye} / C_b < 0.5$) used in Section 3.2. The level of wall boundary transverse reinforcement provided is also used as a basis for categorizing the coupling beam force-deformation behavior, with categories of SBE (special boundary element satisfying ACI 318-11 Section 21.9.6.4), OBE (ordinary boundary element satisfying ACI 318-11 Section 21.9.6.5(a) with $\rho > 400/f_y$), or Other (no special or ordinary boundary element with $\rho \leq 400/f_y$).

Section 3 recommendations, based on the test results of Motter et al (2013) which did not include auxiliary transfer bars and bearing plates, are not intended to be used where auxiliary transfer bars and bearing plates are provided. If auxiliary transfer bars and/or bearing plates are used with shear-yielding members, the test results of Gong and Shahrooz (2001a,b) may be used to determine modeling parameters.

3.1.7

Concrete Encasement Detailing (Section 2.7): No modification.

C3.1.7

The recommended detailing for concrete encasement is intended to provide consistency with ACI 318-11 requirements for diagonally-reinforced concrete coupling beams.

3.2 Modeling and Behavior Categories

3.2.1

Modeling recommendations for flexure-controlled SRC coupling beams with $2 \leq (\alpha = L/h) \leq 4$ are defined for three behavior categories in Table 3.1.

Table 3.1: Summary of Behavior Categories

Category		$A_s f_{ye} / C_b$	Wall Boundary Transverse Reinf.	Maximum Chord Rotation	% of $V_{ne,limit}$ used to Compute L_e	Modeling
I	A	≥ 1.0	SBE, OBE ¹	0.06	100%	SRC1
					80%	SRC2
	B		Other ²	0.03	100%	SRC1
					80%	SRC2
II	A	$\geq 0.5 \ \& \ < \ 1.0$	SBE, OBE ¹ , Other ²	0.06	100%	SRC3
					80%	SRC4
	B	< 0.5		0.03	100%	SRC3
					80%	SRC4
III		< 0.5	SBE, OBE ¹ , Other ²	0.06	100%	SRC4

1: satisfies ACI 318-11 Section 21.9.6.5 with $\rho > 400/f_y$

2: satisfies ACI 318-11 Section 21.9.6.5 with $\rho \leq 400/f_y$

Category I:

- (A): Where sufficient wall longitudinal reinforcement across the embedment length exists ($A_s f_{ye} / C_b \geq 1.0$) and wall boundary transverse reinforcement is classified as either SBE (special boundary element, satisfying ACI 318-11 Section 21.9.6.4) or OBE (ordinary boundary element with 8" maximum vertical spacing of hoops and crossties, satisfying ACI 318-11 Section 21.9.6.5 with the longitudinal boundary reinforcement ratio, ρ , greater than $400/f_y$), the maximum chord rotation for the mean value from the nonlinear response history analyses is 0.06. Minor cyclic degradation and pinching must

be considered; specifically, modeling is based on SRC1 (Appendix B) when $V_{n,embed} \geq V_{ne,limit}$ and SRC2 when $V_{n,embed} \geq 0.8*V_{ne,limit}$.

- (B): Where sufficient wall longitudinal reinforcement across the embedment length exists ($A_s f_{ye}/C_b \geq 1.0$) and wall boundary transverse reinforcement is classified as “Other” (neither SBE nor OBE, satisfying ACI 318-11 Section 21.9.6.5 with $\rho \leq 400/f_y$), the maximum chord rotation for the mean value from the nonlinear response history analyses is 0.03. Minor cyclic degradation and pinching must be considered; specifically, modeling is based on SRC1 (Section 7.2) when $V_{n,embed} \geq V_{ne,limit}$ and SRC2 (Appendix B) when $V_{n,embed} \geq 0.8*V_{ne,limit}$.

Category II:

- (A): Where modest wall longitudinal reinforcement across the embedment length exists ($0.5 \leq A_s f_{ye}/C_b < 1.0$) the maximum chord rotation for the mean value from the nonlinear response history analyses is 0.06, regardless of the classification of the wall boundary transverse reinforcement. For this case, strength is lower than for Category I and significant cyclic degradation and pinching must be considered; specifically, modeling is based on SRC3 (Section 7.2) when $V_{n,embed} \geq V_{ne,limit}$ and SRC4 (Appendix B) when $V_{n,embed} \geq 0.8*V_{ne,limit}$.
- (B): Where light wall longitudinal reinforcement across the embedment length exists ($A_s f_{ye}/C_b < 0.5$), the maximum chord rotation for the mean value from the nonlinear response history analyses is 0.03, regardless of the classification of the wall boundary transverse reinforcement. For this case, strength is lower than for Category I and modest cyclic degradation and pinching must be considered; specifically, modeling is based on

SRC3 (Section 7.2) when $V_{n,embed} \geq V_{ne,limit}$ and SRC4 (Appendix B) when $V_{n,embed} \geq 0.8*V_{ne,limit}$.

Category III:

- Where light wall longitudinal reinforcement across the embedment length exists ($A_{s,lye}/C_b < 0.5$), the maximum chord rotation for the mean value from the nonlinear response history analyses is 0.06, regardless of the classification of the wall boundary transverse reinforcement. For this case, strength is lower than for Category I and Category II and significant cyclic degradation and pinching must be considered; specifically, modeling is based on SRC4 (Appendix B) when $V_{n,embed} \geq V_{ne,limit}$.

C3.2.1

The test results (Motter et al, 2013) reported in Table B.1, along with reported load-deformation behavior (beam shear force vs. beam chord rotation hysteresis loops) in Figure B.1, were used to develop three behavior categories for SRC beams. The three categories describe SRC beams with robust force-deformation behavior with the highest strength and little-to-no cyclic degradation or pinching (Category I), lower strength and modest-to-significant cyclic degradation and pinching (Category II), and even lower strength with significant cyclic degradation and pinching (Category III). Appropriate modeling parameters for each category are described. Assignment of a particular SRC beam into one of the three categories depends on the SRC coupling beam attributes (e.g., quantities of wall longitudinal and transverse boundary reinforcement and coupling beam chord rotation demands). The intent

of the recommendations is to allow all SRC coupling beam behavior categories in a given building, provided that appropriate modeling parameters are used.

Use of a ratio of $A_s f_y / C_b$ less than one is not allowed for prescriptive design (Equation (2.14)). However, a lower ratio is permitted for Category II and Category III for alternative design since the reduced strength and increased cyclic degradation relative to Category I are considered in the modeling parameters.

While stiffness parameters could be selected for the various behavior categories based on Table B.2 in Appendix B, stiffness values depend modestly on wall loading (Motter et al, 2013). Because the wall demands will vary over the wall height at locations where coupling beams exist (due to structural geometry, spatial layout of lateral force resisting elements, etc.), the use of an effective stiffness determined based on the prescriptive recommendations in Section 2.4 (with modification for expected material properties per Section 3.4.1) is recommended, as this is essentially an average value for stiffness obtained from the test results of Motter et al (2013).

It is noted that conditions for Category I (A) are most likely to exist for beams at low-to-mid levels of the building, while conditions for Category I (B) are most likely to exist for beams at low-to-mid level stories, and might exist at upper levels. Conditions for Category II (A) are most likely to exist at mid-to-upper level stories of a building, while conditions for Category II (B) and Category III are most likely to exist at upper level stories.

3.2.2

In accordance with Section 3.1.5 and Section 2.5.1, the minimum required embedment length shall be determined based on capacity design using the upper bound SRC beam strength, $V_{ne,limit}$, unless the full embedment length may not be provided due to geometric constraints (use of a smaller steel section would eliminate this problem). However, in no case shall the embedment strength be less than $0.80V_{ne,limit}$. If a reduced embedment length is used, lower strength and increased cyclic degradation and pinching shall be considered in the model (modeling based on SRC2 rather than SRC1 for Category I and SRC4 rather than SRC3 for Category II, with reference to Section 3.2.1 and Appendix B).

C3.2.2

Although the tests conducted by Motter et al (2013) used reduced embedment lengths in some cases to test limiting conditions, the consistent use of a reduced embedment length represents poor practice, as reduced embedment strength leads to reduced performance, characterized by increased pinching and cyclic degradation. The use of a reduced embedment length is not recommended but is permitted in order to address conditions where use of the full length is not practical due to configuration constraints.

3.3 Wall Demands

3.3.1

For at least 80% of all SRC coupling beams over the building height, either wall boundary longitudinal reinforcement strains, $\varepsilon_{s,bl}$, shall be limited to

$$\varepsilon_{s,bl} \leq 2\varepsilon_y \quad (3.1)$$

or wall plastic rotations, $\theta_{p,bl}$, shall be limited to

$$\theta_{p,bl} \leq 1.2\theta_{y,w} \quad (3.2)$$

where $\varepsilon_{s,bl}$ and $\theta_{p,bl}$ are computed as the mean of the maximum for the building model subjected to the requisite number of base acceleration histories, ε_y is taken as the yield strain of wall boundary longitudinal reinforcement, and $\theta_{y,w}$ is taken as the yield rotation of the wall.

C3.3.1

The modeling parameters for the behavior categories (Section 3.2) were developed with an understanding that local yielding above the wall base (plastic hinge) is likely to occur at a limited number of locations. This local yielding is likely due to higher mode impacts on wall moment and typically will occur at locations where moment strength changes due to cut-offs of wall boundary longitudinal reinforcement, significant changes in the quantity of wall web longitudinal reinforcement, or a reduction in wall cross section. To ensure “essentially elastic”

behavior, the PEER/ATC 72-1 (2010) report recommends that yielding in the upper levels of the wall be limited to tensile strains that do not exceed twice the yield strain or plastic rotations that do not exceed 1.2 times the yield rotation. In satisfying Equation (3.1) or Equation (3.2) for 80% of all SRC coupling beams over the building height, wall strains exceeding $2\varepsilon_y$ or plastic rotations exceeding $1.2\theta_{y,w}$, respectively, would not occur for more than 20% of the SRC coupling beams. Adopting different modeling parameters at locations where tension strains exceed $2\varepsilon_y$ or plastic rotations exceed $1.2\theta_{y,w}$ would not significantly change response results such as lateral story displacements, coupling beam chord rotations, and wall shears; therefore, a less complex modeling approach is adopted.

APPENDIX A. SAMPLE COMPUTATION FOR FLEXURAL STRENGTH

A sample calculation for a 24"x36" SRC coupling beam containing an embedded W24x250 illustrates the computation of the nominal plastic flexural strength, M_p . 6-ksi specified compressive strength of concrete (f'_c) and 50-ksi specified minimum yield strength of structural steel (F_y) was assumed for this example. M_p is determined based on plastic section analysis, in which the plastic steel stress is taken as the specified minimum yield strength of structural steel, F_y , and concrete in compression is modeled with a uniform magnitude (Whitney) stress block (consistent with the stress and force diagram shown in Figure A.1). In practice, iteration must be used to determine the neutral axis depth, x , to satisfy internal force equilibrium, and for the case of this example, the neutral axis depth was determined through iteration (not shown). In the computations provided, equilibrium of internal forces is checked, and the moment strength of the section is computed.

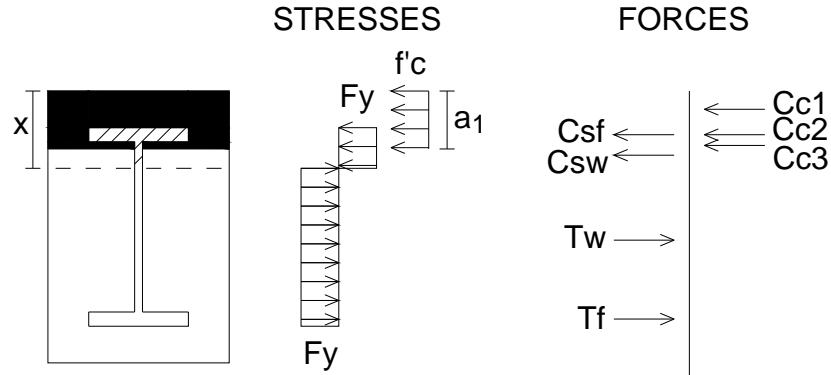


Figure A.1. Stresses and Forces on Cross-Section for Plastic Analysis

$$x = 10.24$$

$$a_1 = \beta_1 x = (0.75)(10.24") = 7.68"$$

$$T_f = A_f F_y = (13.2")(1.89")(50.0^{ksi}) = 1247^k$$

$$T_w = (h - \text{cover} - t_f - x)t_w F_y = (36" - 4.85" - 1.89" - 10.24")(1.04")(50.0^{ksi}) = 989^k$$

$$\sum T = 2236^k$$

$$C_{s_f} = T_f = 1247^k$$

$$C_{s_w} = (x - t_f - \text{cover})t_w F_y = (10.24" - 1.89" - 4.85")(1.04")(50.0^{ksi}) = 182^k$$

$$C_{c_1} = 0.85 f'_c (\text{cover}) b = 0.85(6^{ksi})(4.85")(24") = 594^k$$

$$C_{c_2} = 0.85 f'_c t_f (b - b_f) = 0.85(6^{ksi})(1.89")(24" - 13.2") = 104^k$$

$$C_{c_3} = 0.85 f'_c (a_1 - t_f - \text{cover})(b - t_w) = 0.85(6^{ksi})(7.68" - 1.89" - 4.85")(24" - 1.04") = 110^k$$

$$\sum C = 2237^k$$

$$\sum T = \sum C \rightarrow \text{OK, EQUILIBRIUM}$$

Summing moments about the neutral axis determines the flexural strength as follows:

$$M_{T_f} = T_f * \left(h - \text{cover} - \frac{t_f}{2} - x \right) = 1247^k * \left(36'' - 4.85'' - \frac{1.89''}{2} - 10.24'' \right) = 24896^{k-in}$$

$$M_{T_w} = T_w * \frac{(h - \text{cover} - t_f - x)}{2} = 989^k * \frac{(36'' - 4.85'' - 1.89'' - 10.24'')}{2} = 9405^{k-in}$$

$$M_{C_{s_f}} = C_{s_f} * \left(x - \text{cover} - \frac{t_f}{2} \right) = 1247^k * \left(10.24'' - 4.85'' - \frac{1.89''}{2} \right) = 5543^{k-in}$$

$$M_{C_{s_w}} = C_{s_w} * \frac{(x - \text{cover} - t_f)}{2} = 182^k * \frac{(10.24'' - 4.85'' - 1.89'')}{2} = 319^{k-in}$$

$$M_{C_{c_1}} = C_{c_1} * \left(x - \frac{\text{cover}}{2} \right) = 594^k * \left(10.24'' - \frac{4.85''}{2} \right) = 4642^{k-in}$$

$$M_{C_{c_2}} = C_{c_2} * \left(x - \text{cover} - \frac{t_f}{2} \right) = 104^k * \left(10.24'' - 4.85'' - \frac{1.89''}{2} \right) = 462^{k-in}$$

$$M_{C_{c_3}} = C_{c_3} * \left(x - a_1 + \frac{(a_1 - \text{cover} - t_f)}{2} \right) = 110^k * \left(10.24'' - 7.68'' + \frac{(7.68'' - 4.85'' - 1.89'')}{2} \right) = 333^{k-in}$$

$$M_p = \sum M = 45600^{k-in} = 3800^{k-ft}$$

APPENDIX B. TEST RESULTS AND BACKBONE MODELING

B.1 Summary of Test Parameters

Table B.1 provides a summary of some important test parameters for the four flexure-yielding beams, SRC1 to SRC4, tested by Motter et al (2013). All parameters in Table B.1 were computed based on as-tested material properties with $V_{n,embed}$ and C_b computed based on the provided embedment length (and $V_{ne,limit}$ taken as $V@M_{pe}$ in the computation of C_b). $\epsilon_{s,max}$ is the analytically-determined maximum tensile strain on the outermost wall boundary longitudinal reinforcement at the location of the coupling beam centerline. $\epsilon_{s,max}$ was determined based on plane-section analysis of the structural wall section for the observed maximum applied wall demands during testing, noting that the effect of the local coupling beam bearing forces was not considered in this analysis (i.e., the impact of the bearing forces on the plane section assumption is neglected). ϵ_y is the yield strain of the wall boundary longitudinal bars based on the as-tested material properties.

Table B.1: Test Parameters Used to Determine Behavior Categories

Test Beam	$V@M_{pe}$ (kips)	$V_{n,embed}$ (kips)	C_b (kips)	$V_{n,embed} /$ $V@M_{pe}$	$A_s f_{ye} /$ C_b	Wall $\epsilon_{s,max} / \epsilon_y$	Wall Bound. Trans. Reinf.
SRC1	184.5	189.2	340.3	1.03	1.49	0.41	OBE ¹
SRC2	184.5	119.1	435.6	0.65	1.40	0.70	OBE ¹
SRC3	245.2	146.5	457.6	0.60	0.62	1.06	OBE ¹
SRC4	174.8	105.2	457.2	0.60	0.26	0.50	Other ²

1: satisfies ACI 318-11 Section 21.9.6.5 with $\rho > 400/f_y$

2: satisfies ACI 318-11 Section 21.9.6.5 with $\rho \leq 400/f_y$

In Table B.1, normalized values are provided for embedment strength, strength of wall boundary longitudinal reinforcement crossing the embedment length, and wall demands. Specifically,

$V_{n,embed}/V@M_{pe}$ is intended to assess the level of embedment provided, $A_s f_{ye}/C_b$ is intended to assess the quantity of wall reinforcement provided across the embedment length, and $\varepsilon_{s,max}/\varepsilon_y$ is intended to assess the level of the applied maximum wall demands. The quantity of wall boundary transverse reinforcement provided is categorized as SBE, OBE, or Other. Referring to ACI 318-11, a special boundary element (SBE) satisfies Section 21.9.6.4, an ordinary boundary element (OBE) satisfies Section 21.9.6.5 with the longitudinal boundary reinforcement ratio greater than $400/f_y$, and conditions for no boundary element (Other) satisfy Section 21.9.6.5 with the longitudinal boundary reinforcement ratio less than or equal to $400/f_y$.

B.2 Modeling

The plots in Figure B.1 show the load-displacement response, the corresponding first- and second-cycle backbone curves (from test data), and a backbone model for each of the four test beams (Motter et al, 2013). First- and second-cycle backbone curves were included as a means to assess cyclic degradation. The first-cycle backbone is indicative of peak responses, whereas the second-cycle backbone is more indicative of reliable strength conditions. The model backbones were based on curve-fitting to the second-cycle backbone relation. Specifically, in each (positive and negative) direction, the strength along the yield plateau was computed as the average value between 2% and 6% rotation, and the elastic stiffness was computed based on interpolating a displacement from the backbone curve at a load equal to two-thirds of the load associated with the yield plateau. Post-peak strength degradation was modeled to be linear after 6% rotation, and the final point on each backbone model corresponds to the final point on the second-cycle backbone curve for each test. Note that a minor variation to this curve-fitting

procedure was made for SRC3 in the positive loading direction. Due to the strength increase for SRC3 beyond 6% rotation in the positive loading direction, the strength along the yield plateau was computed as the average value between 2% and the final point on the second-cycle backbone curve. Note that alternative bilinear backbone curves could be developed to avoid modeling strength degradation.

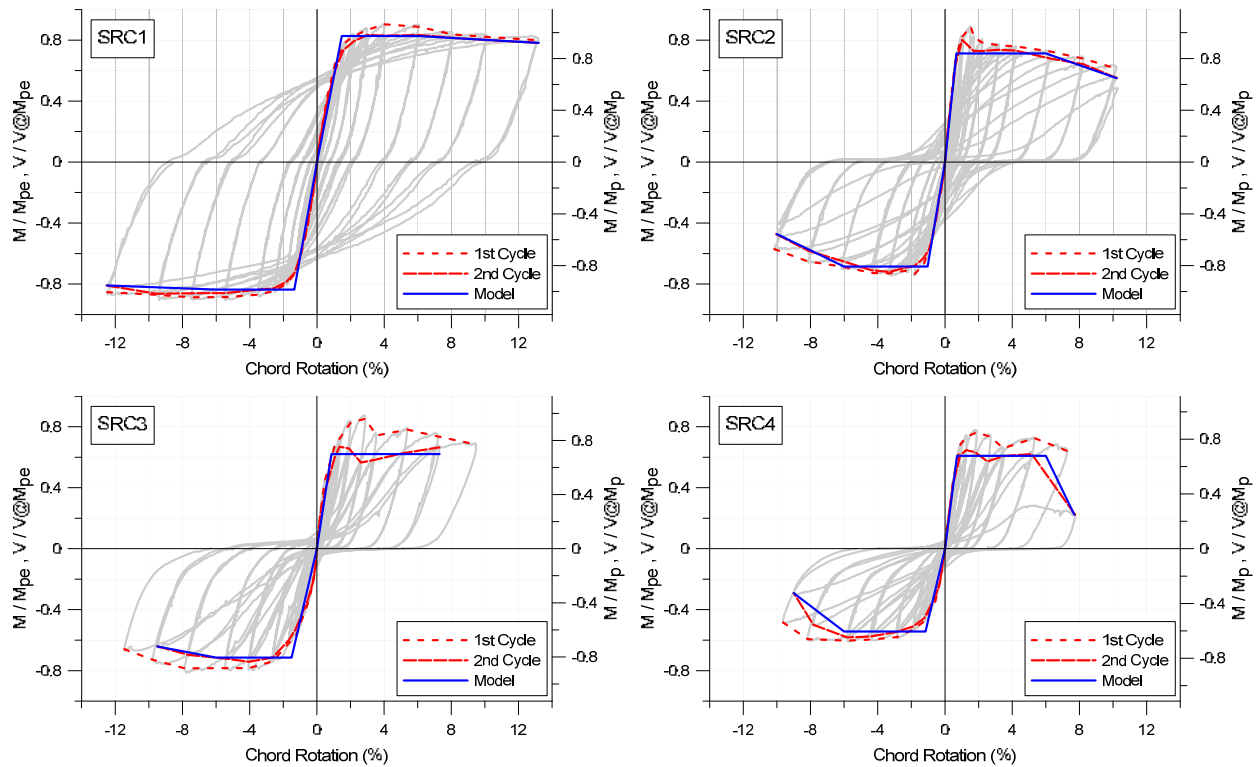


Figure B.1. Backbone Modeling of Load-Displacement Response

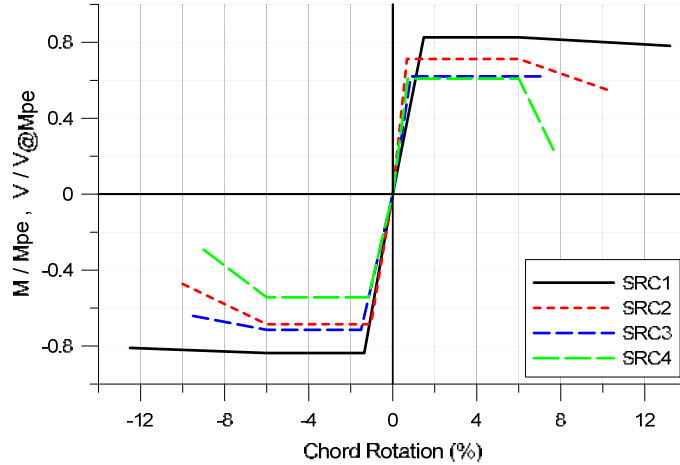


Figure B.2. Comparison of Backbone Models for All Test Beams

Figure B.2 shows the backbone models for all test beams, in order to highlight the differences in beam performance. Figure B.3 illustrates five variables, namely A_1 , A_2 , B_1 , C_1 , and D_1 , used to define the backbone models in Figure B.1 and Figure B.2. A_1 is the effective rotational stiffness, expressed as a fraction of M_{pe}/rad or $V@M_{pe}/\text{rad}$, when modeling a rigid beam span with rotational springs at the beam-wall interfaces (a concept discussed in Section 2.4, where the spring stiffness K represents the stiffness term A_1). Alternatively, A_2 is the equivalent effective bending stiffness, expressed as a fraction of $\alpha E_s I_{trans}$ (noting that α was 3.33 for SRC1, SRC2, and SRC4 and 2.4 for SRC3, where I_{trans} is based on E_c , computed using the as-tested compressive strength of concrete, $f'_{c,test}$), when using a lumped deformation approach in which all deformations are modeled as flexure within the beam span (i.e. when modeling a rigid shear stiffness with no rotational springs at the beam-wall interfaces). B_1 is the strength along the backbone yield plateau, expressed as a fraction of M_{pe} or $V@M_{pe}$ (with M_{pe} and $V@M_{pe}$ computed in accordance with Section 6.2.1). C_1 indicates the strength drop (also expressed as a fraction M_{pe} or $V@M_{pe}$) occurring after a chord rotation of 0.06 radians, and D_1 (in radians) indicates the rotation beyond 0.06 radians over which this linear strength drop occurs.

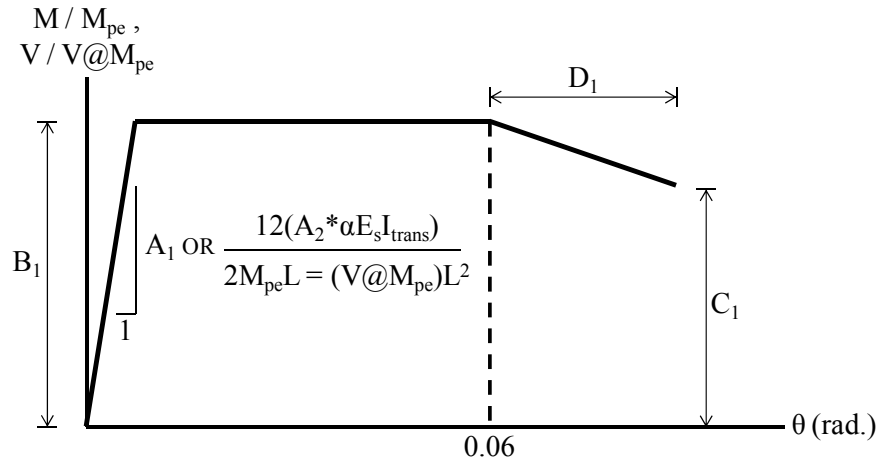


Figure B.3. Parameters Used to Define Backbone Models

Table B.2: Backbone Modeling Parameters for All Test Beams

Test Beam	Sign	A_1	A_2	B_1	C_1	D_1
SRC1	(+)	58	0.048	0.83	0.78	0.072
	(-)	63	0.053	0.84	0.81	0.065
SRC2	(+)	107	0.090	0.71	0.55	0.042
	(-)	66	0.055	0.69	0.47	0.040
SRC3	(+)	74	0.063	0.62	0.62	0.013
	(-)	47	0.040	0.71	0.64	0.035
SRC4	(+)	88	0.075	0.61	0.22	0.017
	(-)	47	0.040	0.54	0.29	0.030

Similar to the tables found in ASCE Standard 41-06 for conventional and diagonally-reinforced coupling beams, Table B.2 summarizes the values of A_1 , A_2 , B_1 , C_1 , and D_1 for each of the backbone models shown in Figure B.1 and Figure B.2. Although the values of A_1 , A_2 , B_1 , C_1 , and D_1 in Table B.2 differ in the positive and negative loading directions due to asymmetry in the observed load-displacement responses, the backbone models used for alternative analysis in Section 3.2 may be based on average values (Figure B.4 and Table B.3). Specifically, values of $A_1 = 75$ and $A_2 = 0.06$ in Table B.3, which were used to formulate the stiffness recommendations provided in Section 3.1.4 and Section 2.4, were based on the average of all values shown in

Table B.2, while the values for B_I , C_I , and D_I in Table B.3 were based on the average of the positive and negative values shown in Table B.2 for each beam. Further discussion on the use of average values is provided in the following paragraph.

While stiffness parameters could be selected for the various behavior categories based on Table B.2, stiffness values depend modestly on wall loading (Motter et al, 2013). Because the wall demands will vary over the wall height at locations where coupling beams exist (due to structural geometry, spatial layout of lateral force resisting elements, etc.), the use of an average stiffness is recommended. Given that the load-displacement asymmetry was relatively modest (Figure B.2 and Table B.2) and that beam shear in full-length coupling beams (as opposed to one-half-length cantilever test beams) would be based on the average of the positive and negative moments that develop at each end of the beam (i.e. the inflection point is not at the center of the clear span if the magnitude of the member end moments differ), use of average values is recommended and should be used when modeling is performed with a shear force - displacement/rotation backbone (as opposed to a moment-rotation backbone).

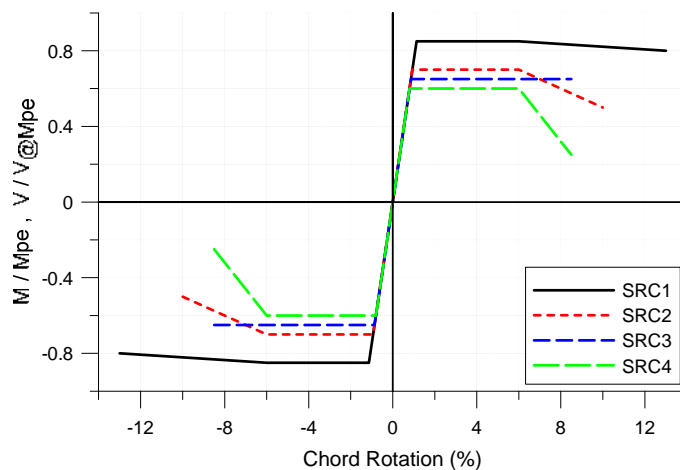


Figure B.4: Backbone Models for Alternative Analysis

Table B.3: Backbone Modeling Parameters for Alternative Analysis

Test Beam	A_1	A_2	B_1	C_1	D_1
SRC1	75	0.06	0.85	0.80	0.070
SRC2			0.70	0.50	0.040
SRC3			0.65	0.65	0.025
SRC4			0.60	0.25	0.025

Nonlinear modeling of buildings using alternative analysis is typically conducted with the assistance of computer software, such as CSI Perform 3D (2011). In Perform 3D, using shear-displacement hinges or moment-rotation hinges, which include the optional use of cyclic degradation energy factors (which range between zero and one, with larger values corresponding to broader hysteretic loops, i.e., less pinching) to specify the degree of pinching in the load-deformation relations, is appropriate for modeling the nonlinear response of coupling beams. For each test beam (Motter et al, 2013), the cyclic degradation energy factors provided in Table B.4 and the backbone parameters in Table B.3 were used in Perform 3D (Figure B.5) to produce the modeling results in Figure B.6. To better match the shape of the hysteretic loops, the backbone models shown in Figure B.4 were modified slightly in Perform 3D. Specifically, a trilinear rather than bilinear (elastic-perfectly-plastic) relationship was used in Perform 3D (Figure 7.5). In this trilinear relationship, the yield strength was taken as 95% of the ultimate strength ($DY/DU = 0.95$ in Figure 7.5, with ultimate strength indicated by parameter B_1 in Table B.3) and the rotation at which peak strength is reached was taken as 0.055 radians ($DU = 0.055$ in Figure B.5), consistent with the modeling approach used by Naish et al (2009). The cyclic degradation energy factors (Table B.4 and Figure B.5) were selected in order to achieve roughly equivalent energy dissipation (Figure B.7 and Figure B.8) between the model relations and the test beam relations over the range of rotations typically expected for coupling beams (i.e., up to

about 6% chord rotation, as discussed in Motter et al, 2013). Due to the limitations of the cyclic degradation modeling parameters in Perform 3D, accurate modeling of energy dissipation over this range of rotations led to an underestimate of energy dissipation at rotations beyond this range in certain instances (Figure B.7 and Figure B.8). In comparing the shear-displacement hinge (V-Hinge) versus moment-rotation hinge (M-Hinge) modeling results for each specific test beam (Figure B.6), it is noted that use of the Unloading Stiffness Factor, which is available with a moment-rotation hinge but not with a shear-displacement hinge in Perform 3D, improves the shape of the hysteretic loops (Figure B.6). Despite the difference in the shape of the hysteretic loops, the difference in energy dissipation between the M-Hinge model (Figure B.7) and V-hinge model (Figure B.8) is negligible.

Table B.4: *Perform 3D Cyclic Degradation Parameters for Alternative Analysis*

Test Beam	Y	U	L	R	X	Unloading Stiffness Factor *
SRC1	0.40	0.40	0.40	0.40	0.40	1.0
SRC2	0.40	0.40	0.40	0.20	0.20	1.0
SRC3	0.20	0.20	0.20	0.20	0.20	1.0
SRC4	0.20	0.15	0.15	0.15	0.15	1.0

* available with moment-rotation hinge, unavailable with shear-displacement hinge

COMPONENT PROPERTIES

Materials | Strength Sects | Compound

Inelastic | Elastic | Cross Sects.

Type: Moment Hinge, Rotation Type

New Choose type and name to edit an existing component.

Name: Nonlinear Backbone

Purge | Rename | Text for filter. | Filter

Length Unit: in | Force Unit: kip

Status: Old property set. Changed. Not yet checked.

Check | Save | Save As | UnChange

Shape of Relationship: E-P-P | Trilinear

Use Cross Section: Yes | No

Symmetry: Yes | No

Deformation Capacities: Yes | No

Strength Loss: Yes | No

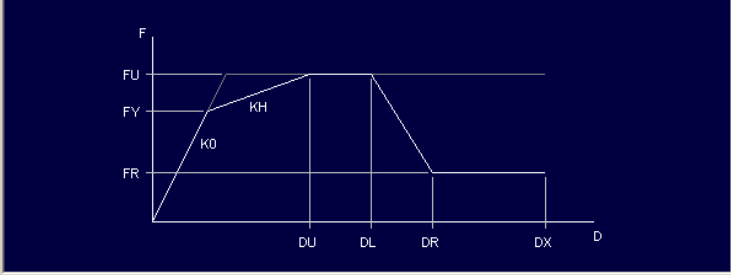
Upper/Lower Bounds: Yes | No

Cyclic Degradation: None | YULRX | YX+3

Import Components | Export Components

Selected components of this type. | Import ...

All components of all types.



Section and Dimensions | Basic F-D Relationship | Strength Loss

Deformation Capacities | **Cyclic Degradation** | Upper/Lower Bounds

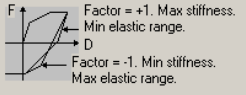
Deformations = hinge rotations

For Positive Deformations		For Negative Deformations	
Point	Energy Factor	Point	Energy Factor
Y	0.4	Y	
U	0.4	U	
L	0.4	L	
R	0.4	R	
X	0.4	X	

Unloading Behavior

Unloading Stiffness Factor: 1 (Min -1, Max +1)

This factor controls the unloading behavior for a trilinear F-D relationship. You can use Plot Loops to show the effect. See the User Guide for details.



Factor = +1. Max stiffness. Min elastic range.

Factor = -1. Min stiffness. Max elastic range.

Paste | Copy | Clear

Figure B.5: Screenshot of Perform 3D Modeling Input

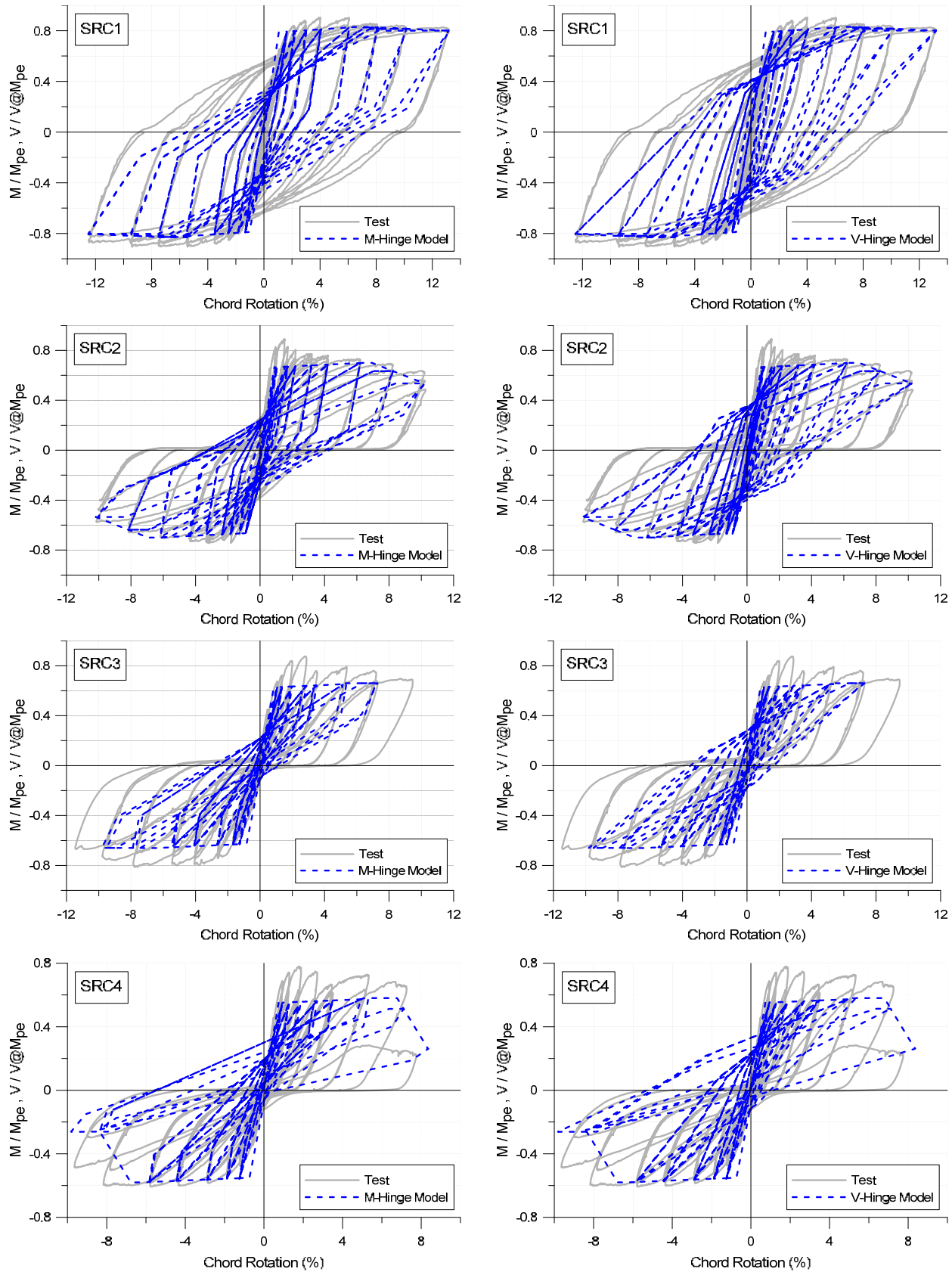


Figure B.6: Perform 3D Modeling of Load-Displacement Response for Each Test Beam

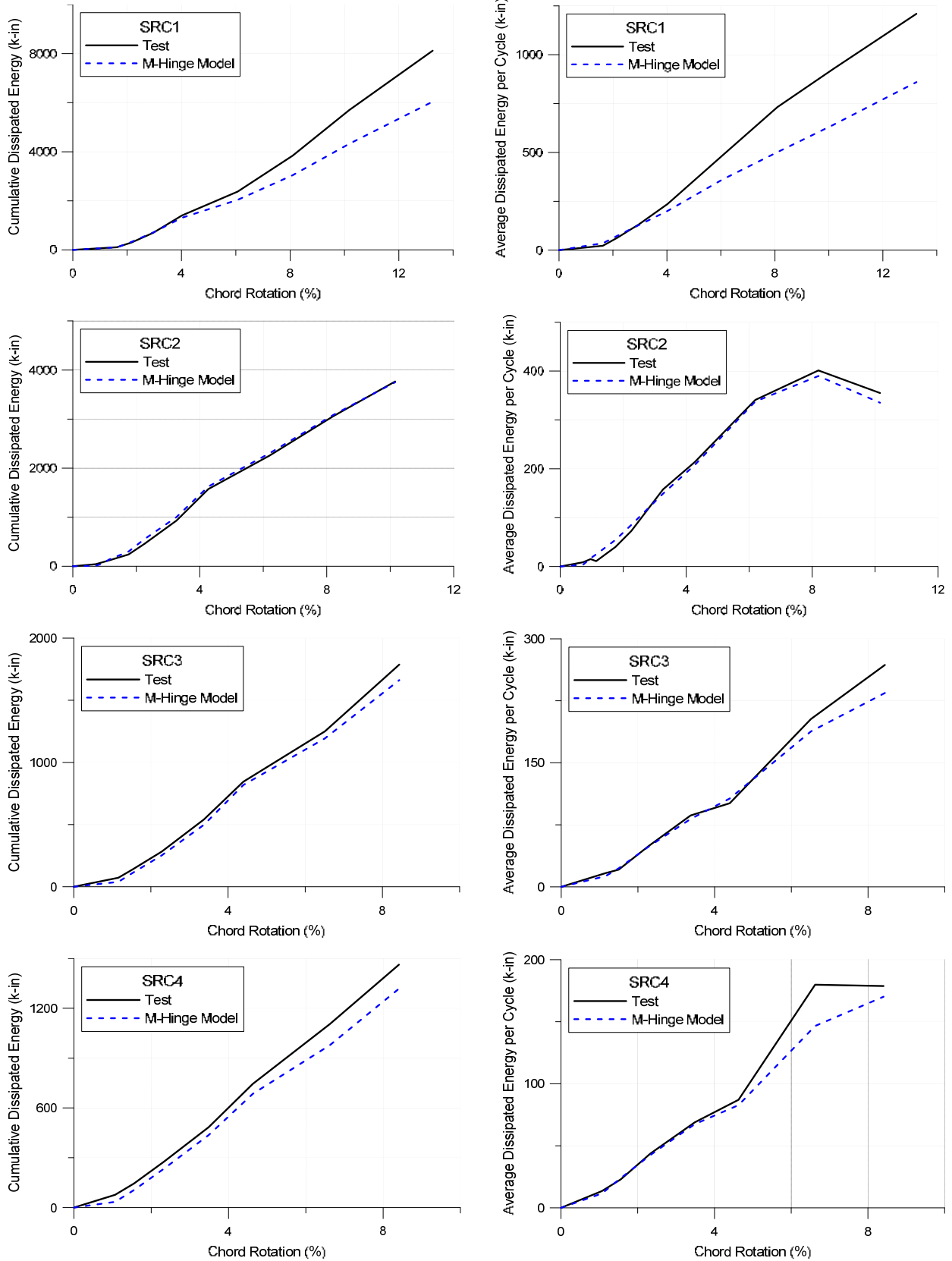


Figure B.7: Dissipated Energy for Test Beams and Perform 3D M-Hinge Models

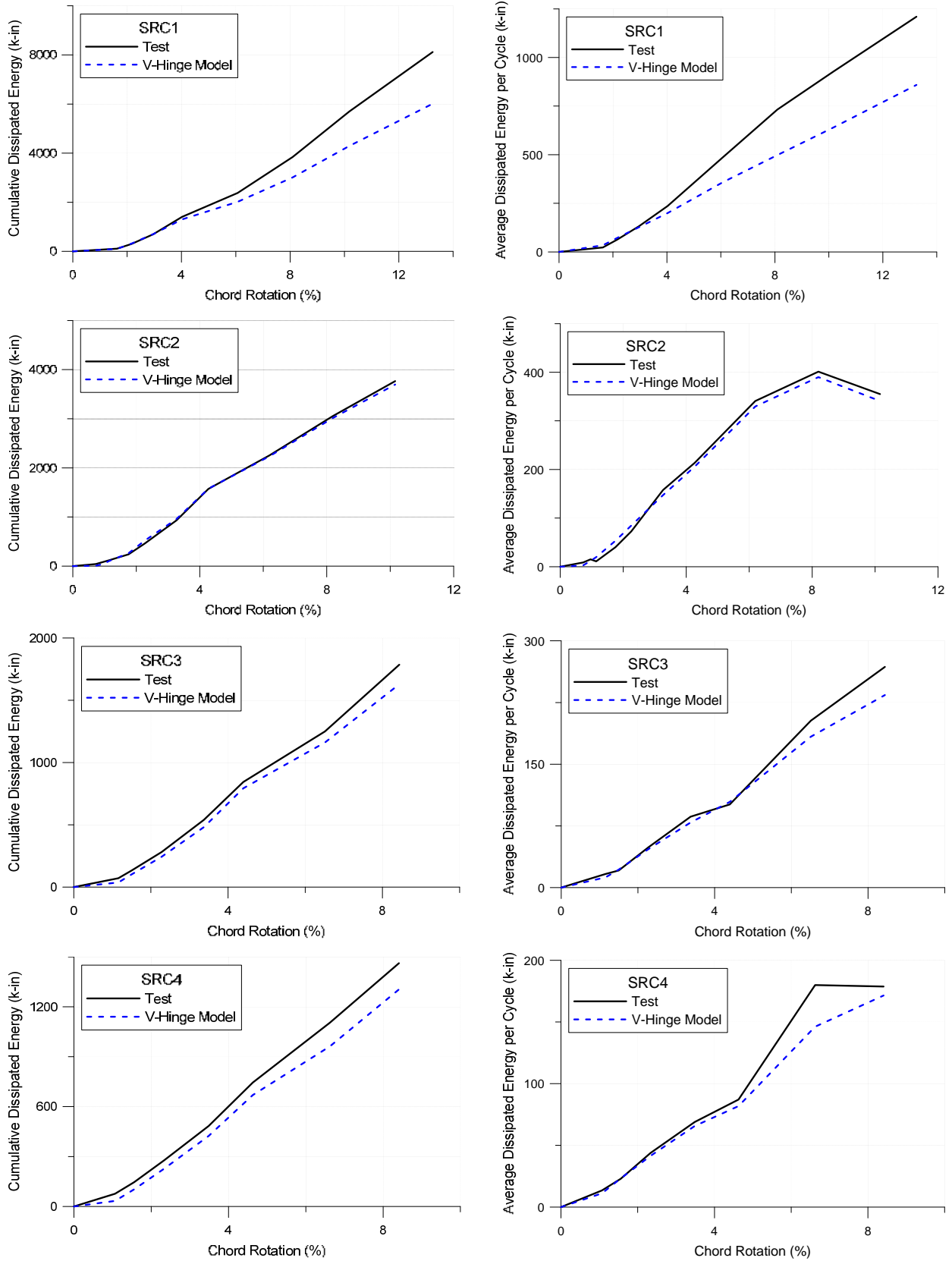


Figure B.8: Dissipated Energy for Test Beams and Perform 3D V-Hinge Models

REFERENCES

- ACI Committee 318. (2011). Building Code Requirements for Structural Concrete (ACI 318-11) and Commentary, American Concrete Institute, Farmington Hills, MI.
- AISC. (2010). Seismic Provisions for Structural Steel Buildings. ANSI/AISC 341-05, American Institute of Steel Construction, Chicago, IL.
- ASCE. (2007). ASCE/SEI Standard 41-06, Seismic Rehabilitation of Existing Buildings. American Society of Civil Engineers, Reston, VA.
- Computers and Structures, Inc (CSI). (2011). Perform 3D, Nonlinear Analysis and Performance Assessment for 3D Structures User Guide, Version 5. Computers and Structures, Inc., Berkeley, CA.
- Gong, B. and Shahrooz, B.M. (2001a). Concrete-Steel Composite Coupling Beams. I: Component Testing. *Journal of Structural Engineering*. 127:6, 625-631.
- Gong, B. and Shahrooz, B.M. (2001b). Concrete-Steel Composite Coupling Beams. II: Subassembly Testing and Design Verification. *Journal of Structural Engineering*. 127:6, 632-638.
- Harries, K.A. (1995). Seismic Design and Retrofit of Coupled Walls Using Structural Steel. *PhD thesis*, Department of Civil Engineering, McGill University, Montreal, Quebec.
- Harries, K.A., Gong, B. and Shahrooz, B.M. (2000). Behavior and Design of Reinforced Concrete, Steel, and Steel-Concrete Coupling Beams. *Earthquake Spectra*. 16:4, 775-798.
- Harries, K.A., Mitchell, D., Cook, W.D., and Redwood, R.G. (1993). "Seismic Response of Steel Beams Coupling Concrete Walls." *Journal of Structural Engineering*. 119(12), 3611-3629.

- Harries, K.A., Mitchell, D., Redwood, R.G., Cook, W.D., (1997). “Seismic Design of Coupled Walls – A Case for Mixed Construction.” *Canadian Journal of Civil Engineering*. 24, 448-459.
- LATBSDC. (2014). An Alternative Procedure for Seismic Analysis and Design of Tall Buildings Located in the Los Angeles Region. Los Angeles Tall Buildings Structural Design Council, Los Angeles.
- Marcakis, K. and Mitchell, D. (1980). Precast Concrete Connections with Embedded Steel Members. *PCI Journal*. 25:4, 88-116.
- Mattock, A.H. and Gaafar, G.H. (1982). Strength of Embedded Steel Sections as Brackets. *ACI Journal*. 79:9, 83-93.
- Motter, C.J., Fields, D.C., Hooper, J.D., Klemencic, R., and Wallace, J.W. (2013). Large-Scale Testing of Steel Reinforced Concrete (SRC) Coupling Beams Embedded into Reinforced Concrete Structural walls. *UCLA SGEL Research Report*, University of California, Los Angeles.
- Naish, D., Fry, A., Klemencic, R., Wallace, J. (2013a). Reinforced Concrete Coupling Beams – Part I: Testing. *ACI Structural Journal*. 110:6, 1057-1066.
- Naish, D., Fry, A., Klemencic, R., Wallace, J. (2013b). Reinforced Concrete Coupling Beams – Part II: Modeling. *ACI Structural Journal*. 110:6, 1067-1075.
- Naish, D., Wallace, J.W., Fry, J.A. and Klemencic, R. (2009). Reinforced Concrete Link Beams: Alternative Details for Improved Construction. *UCLA – SGEL Report 2009/06*.
- Nowak, A.S., Szerszen, M.M., Szeliga, E.K., Szwed, A., and Podhorecki, P.J. (2008). Reliability-Based Calibration for Structural Concrete, Phase 3. SN2849, Portland Cement Association, Stokie, IL.

PEER/ATC-72-1. (2010). Modeling and Acceptance Criteria for Seismic Design and Analysis of Tall Buildings. Pacific Earthquake Engineering Research Center (PEER) and Applied Technology Council (ATC) Joint Task Force.

PEER Tall Buildings Initiative (TBI). (2010). Guidelines for Performance-Based Seismic Design of Tall Buildings. PEER Report 2010/05, Pacific Earthquake Engineering Research Center (PEER), University of California, Berkeley.

SEAONC AB-083. (2007). Recommended Administrative Bulletin on the Seismic Design and Review of Tall Buildings Using Non-Prescriptive Procedures. Structural Engineers Association of Northern California (SEAONC) AB-083 Tall Buildings Task Group, San Francisco.

Shahrooz, B.M., Remmetter, M.E. and Qin, F. (1993). Seismic Design and Performance of Composite Coupled Walls. *Journal of Structural Engineering*. 119:11, 3291-3309.